Masterarbeit

zur Erlangung des akademischen Grades

Master of Science

im Fach Physik

Estimation and approximation of the nonlinear response of stochastic neuron models with adaptation

eingereicht von: Christoph H. Egerland

Gutachter/innen: 1. Prof. Dr. Benjamin Lindner

2. Prof. Dr. Martin Falcke

Eingereicht am Institut für Physik der Humboldt-Universität zu Berlin am:

"There are no answers, only cross-references."

– Norbert Wiener

Abstract

Neurons, the fundamental building blocks of all information processing in living beings, are fundamentally nonlinear elements. If a neuron receives an input signal, it produces a specific output. However, if the neuron is subject to two signals its output may not be the sum of the specific outputs. This constitutes a violation of superposition or, in other words, it is a sign of nonlinearity.

In this work we show how said nonlinearity helps to describe a real life observation in weakly electric fish, the so-called electrosensory cocktail party, which we will describe in more detail in chapter 1 along with the mathematical framework of this thesis. Using nonlinear systems theory and the Volterra/Wiener series we reduce the problem to the identification of the (higher order) susceptibilities of our system – which are the sensory neurons of the weakly electric fish. The cocktail party effect is especially alluring to us, since the sensory neurons are well described by a leaky integrate-and-fire model with spike-frequency adaptation. For the nonadapting leaky integrate-and-fire neuron we will explore an analytical calculation in chapter 2 which closely follows a previous calculation in Ref. [1, 2].

Then, in chapter 3, we investigate the dependency of the susceptibilities on internal and external parameters of our system. More specifically we will see that the susceptibilities are dependent on the noise that is intrinsic to the neuron as well as to the signal noise.

In chapter 4 we finally introduce the adapting leaky integrate-and-fire model and explore the effects of the adaptation on the firing of the neuron. We find an approximation for which we can analytically calculate the first and second order susceptibilities and show that the results fit well to simulations.

chapter 5 lays out more details on the simulations we performed in the thesis and chapter 6 closes it with a critical discussion of this work.

Zusammenfassung

Neuronen sind, als die kleinsten informationsverarbeitenden Einheiten in Lebenwesen fundamental nichtlineare Elemente. Wenn ein Neuron ein Eingangssignal empfängt, erzeugt es ein spezifisches Ausgangssignal. Wenn es allerdings die Summe aus zwei Eingangssignalen empfängt, dann ist das Ausgangssignal im Allgemeinen nicht gleich der Summe der spezifischen Ausgangssignale. Wir erkennen hierin eine Verletzung des Superpositionsprinzips oder, anders gesagt, ein Zeichen für Nichtlinearität.

In dieser Arbeit zeigen wir wie die genannte Nichtlinearität bei der Beschreibung eines beobachtetes Phänomen in schwach elektrischen Fischen, der sogenannten elektrosensorischen Cocktailparty die wir in Kapitel 1 einführen, helfen kann. Mit Hilfe der Theorie nichtlinearer Systeme und der Volterra- bzw. Wienerreihe reduzieren wir das Problem auf die Identifikation der Suszeptibilitäten unseres Systems (den sensorischen Neuronen des schwach elektrischen Fisches). Der Cocktailpartyeffekt ist für uns von besonderem Interesse, da die sensorischen Neuronen sehr gut durch ein sogenanntes Leckintegratormodell mit stochastischer Adaption beschrieben werden können. Für das Leckintegratormodell ohne Adaption werden wir analytische Ausdrücke in Kapitel 2 berechnen, deren Herleitung sich sehr stark an [1, 2] hält.

In Kapitel 3 werden wir die Abhängigkeit der Suszeptibilitäten von systeminternen und -externen Parametern untersuchen. Spezifischer, werden wir sehen, dass die Suszeptibilitäten von einer Kombination aus intrinsischem und extrinsischen Rauschen abhängen.

In Kapitel 4 führen wir dann das Leckintegratormodell mit stochastischer Adaption ein und erkunden die Effekte der Adaption auf das Feuern des Neurons. Wir werden eine Approximation finden die uns erlaubt analytische Ausdrücke für die Suszeptibilität erster und zweiter Ordnung zu finden und wir zeigen, dass diese Ergebnisse sich mit Simulationen decken.

In Kapitel 5 legen wir Details über die durchgeführten Simulationen dar und in Kapitel 6 beenden wir die Arbeit mit einer kritischen Diskussion.

Contents

CHAPTER 1

Introduction

We present the problem at hand, the cocktail party of weakly electric fish, and specify its intriguing properties. From there we abstract our problem and formulate it anew using nonlinear response theory, where we introduce the most important quantities of this thesis – the (higher order) susceptibilities.

1.1 The electrosensory cocktail party

Gymnotiforms are weakly electric fish that can generate an electric field by discharging an electric organ, which is usually found in the tail of the fish. For the species *Apteronotus albifrons* the generated field is of approximately dipolar structure, quasisinusoidal and in the frequency range of 800-1300Hz [3, 4]. The electric field is disturbed by any surrounding objects (rocks, plants) and other fish. Disturbances of the electric field are picked up by sensory neurons, which allows preying, navigation and communication with other fish. In a communication scenario two fish are within a certain detection range (which in the case of *A. rostratus* is around 1.5m [5]), outside of which the signal of either fish is too weak to be detected. Their electric organ discharges (EOD) overlap, causing an amplitude modulation. This amplitude modulation is picked up by receptors called P-units (probability units), which encode these modulations, meaning that they are more likely to fire if there is a higher amplitude modulation. However, the modulation has to be strong enough to be successfully encoded by the P-unit [6] and there is also a tuning phenomenon, meaning there is a prefered range of frequencies that the P-unit detects. The spiking activity of the P-units is well described by a leaky integrate-and-fire neuron with spike frequency adaptation [6–10] (see chapter 4 for more details on the model).

In [5, 11] they observed an interesting communication scenario involving three fish. A male fish (called the resident) courting a female fish can detect another male fish (called the intruder) at distances that are close to the detection range. This is somewhat stunning, since one expects that a closeby signal would jam the detection of other, especially weak, signals. The described phenomenon is similar to the so-called *cocktail party problem*, which deals with the question: How can the auditory system segragate a signal (the words of a conversation partner) from distracting background sounds (the party)? [12] Therefore our problem is: how can the resident male fish segregate the signal of an intruding male fish, while it is influenced by the signal of a closeby female fish?

Previous works consider the nonlinear response of the leaky integrate-and-fire model together with two input signals [1, 2]. They have shown significant enhancements that can not be explained using linear response. However, they do not consider spike-frequency adaptation, which e.g. has been considered in [13, 14]. In this work we strive to combine the results of

these works to obtain a theory for the nonlinear reponse in an adapting leaky integrate-and-fire model.

Figure 1.1: Black box. We consider an unknown system that takes some time dependent input signal $x(t)$ and produces an output signal $y(t)$.

1.2 Nonlinear systems

We may abstract the fish as a nonlinear system that receives some time dependent input signal $x(t)$ and produces an, also time varying, output signal $y(t)$. It is therefore essentially a black box that is fully determined by its response to the inputs. In mathematical terms we can model such a system using the so-called Volterra series [15]

$$\begin{aligned} y(t) &= H_0[h_0, x(t)] + H_1[h_1, x(t)] + H_2[h_2, x(t)] + \cdots + H_n[h_n, x(t)] \\ &= h_0 + \int_0^\infty d\tau h_1(\tau) x(t-\tau) \\ &+ \int_0^\infty d\tau_1 \int_0^\infty d\tau_2 h_2(\tau_1, \tau_2) x(t-\tau_1) x(t-\tau_2) \\ &+ \dots \\ &+ \int_0^\infty d\tau_1 \cdots \int_0^\infty d\tau_n h_n(\tau_1, \dots, \tau_n) \prod_{i=1}^{n} x(t-\tau_i) \end{aligned} \tag{1.1}$$

where h_i $\{i : i \in [0, n]\}$ are the *Volterra kernels* of ith order and we show a finite Volterra series, but we could also choose infinitely many terms. Knowing all kernels in the Volterra series completely determines the output for a given input. However, there are two new problems that we have to face now. The first is: how many terms do we need? Does the linear order suffice? Do we need infinitely many? We can not answer this question in general, however, in our case we stipulate that the signal is such that we can accurately describe the output using the first three terms of the Volterra series (i.e. zeroth, first and second order). This brings us to the next problem: how do we quantify the kernels? Again, in general this is a hard problem, because (considering only the first three terms) we would have to solve a nonlinear integral equation. There is, however, a way in which we can make progress. A fundamental problem of the Volterra series is, that its terms are not mutually orthogonal with respect to white gaussian noise. Let us consider white gaussian noise with variance A as our input signal and let us

consider the average of the second order term. This results in

$$\langle H_2[h_2, x(t)]\rangle = A\int_0^\infty d\tau h_2(\tau,\tau), \tag{1.2}$$

which is a zeroth order term! We can extend this observation for even higher orders and see that higher order terms contain lower order contributions, leading to a correlation of the different orders. A remedy for this problem has been found by Wiener [16] and is called the Wiener series. It considers as an input a gaussian white noise with variance A and simply substracts the lower order terms that have been causing the correlation from before

$$\begin{aligned} y(t) &= G_0[h_0, x(t)] + G_1[h_1, x(t)] + G_2[h_2, x(t)] + G_3[h_3, x(t)] + \dots \\ &= g_0 + \int_0^\infty d\tau g_1(\tau)x(t-\tau) \\ &+ \int_0^\infty d\tau_1 \int_0^\infty d\tau_2 g_2(\tau_1,\tau_2)x(t-\tau_1)x(t-\tau_2) - A\int_0^\infty d\tau g_2(\tau,\tau) \\ &+ \int_0^\infty d\tau_1 \int_0^\infty d\tau_2 \int_0^\infty d\tau_3 g_3(\tau_1,\tau_2,\tau_3)x(t-\tau_1)x(t-\tau_2)x(t-\tau_3) \\ &- 3A\int_0^\infty d\tau g_3(\tau,\tau,t)x(t-\tau) \\ &+ \dots \end{aligned} \tag{1.3}$$

Here we have only shown the first four terms and we have denoted the *Wiener kernels* with g_i $\{i : i \in [0,n]\}$. Our initial problem was, however, that the measurement of the Volterra kernels is a hard problem. How does the construction of the Wiener series help us? There is a standard way due to Lee and Schetzen [17] that allows an easy (numerical) measurement of the Wiener kernels which is called the cross correlation method. Using this scheme we can easily identify the Wiener kernels. To obtain the appropriate Volterra kernel we then have to use Wiener-to-Volterra formulae [18]. Let us consider a second order Volterra and Wiener series. We set both series equal, since the output $y(t)$ does not depend on the representation we choose. Then we compare each term and we can identify

$$h_0 = g_0 - A\int_0^\infty d\tau g_2(\tau,\tau) \tag{1.4}$$

$$h_1(\tau) = g_1(\tau) \tag{1.5}$$

$$h_2(\tau_1,\tau_2) = g_2(\tau_1,\tau_2). \tag{1.6}$$

In this scenario, only the static (i.e. the zeroth order) term changes depending on the representation we choose.

Later on we will often work with the Fourier transform of the Wiener or Volterra series, which involves the Fourier transforms of the kernels, which are called susceptibilities and – for

the lowest two orders – are defined as follows

$$\chi_1(\omega) = \int_{-\infty}^{\infty} d\tau e^{i\omega\tau} g_1(\tau) \tag{1.7}$$

$$\chi_2(\omega_1, \omega_2) = \int_{-\infty}^{\infty} d\tau_1 e^{i\omega_1\tau_1} \int_{-\infty}^{\infty} d\tau_2 \; e^{i\omega_2\tau_2} g_2(\tau_1, \tau_2), \tag{1.8}$$

which are of course *Wiener susceptibilities*. For the *Volterra susceptibilities* simply replace g with h in the above expressions. Notice that in this thesis we use the following Fourier transform convention

$$f(\omega) = \int_{-\infty}^{\infty} dt f(t) e^{i\omega t} \tag{1.9}$$

$$f(t) = \int_{-\infty}^{\infty} \frac{d\omega}{2\pi} f(\omega) e^{-i\omega t}. \tag{1.10}$$

Using this convention the Wiener series up to second order reads

$$\begin{aligned} r(\omega) = &\left(2\pi r_0 - 2\pi A \int d\omega' \chi_2(\omega', -\omega') \right) \delta(\omega) + \chi_1(\omega) s(\omega) \\ &+ \frac{1}{2\pi} \int d\omega' \chi_2(\omega - \omega', \omega') s(\omega - \omega') s(\omega'). \end{aligned} \tag{1.11}$$

As we can see the static response is encoded by a delta function at $\omega = 0$ which, at first glance, seems problematic. However, it simply represents the fact that we considered the Fourier transform of a nonzero average quantity and can therefore be removed by considering a scaled version of the firing rate. In the Fourier domain the linear response becomes a simple product, while the second order response still involves an integral. This makes calculations involving higher orders hard, which we will see in chapter 4.

CHAPTER 2

Second order susceptibility of general integrate-and-fire neurons

We calculate the first and second order susceptibility for a general integrate-and-fire neuron. A calculation for the specific case of a leaky integrate-and-fire neuron has already been performed in [1, 2] and will serve firstly as the outline for our calculation and secondly as a consistency check.

2.1 Fokker-Planck-Equation and Ansatz

We inspect a general integrate-and-fire neuron, which obeys the following dynamics

$$\tau\dot{v} = f(v) + \varepsilon s(t) + \sqrt{2D}\xi(t), \tag{2.1}$$

where v is the membrane voltage, τ is the membrane time constant, $\varepsilon s(t)$ is an input signal, D is the noise intensity and $\xi(t)$ is gaussian white noise. Additionally we impose a fire-and-reset rule: if the voltage crosses a threshold $v > v_t$ we it to a reset value $v = v_r$ after some refractory period τ_{ref}. If we choose a certain integrate-and-fire neuron we have to specify the drift dynamic, e.g. $f(v) = \mu$ for the perfect integrate-and-fire and $f(v) = \mu - v$ for the leaky integrate-and-fire. An equivalent formulation of the Langevin-type equation for the membrane voltage above is the Fokker-Planck-equation (FPE) for the probability density which in our case reads

$$\partial_t p(v,t) = \underbrace{\partial_v(-f(v) + D\partial_v)}_{:=\hat{L}_0} p(v,t) - \varepsilon s(t)\partial_v p(v,t) + r(t-\tau_{ref})\delta(v - v_r). \tag{2.2}$$

Additionally we have boundary and normalization conditions

$$p(v_t,t) = 0 \qquad \text{absorbing boundary at } v_t \tag{2.3}$$

$$-D\partial_v p(v,t)|_{v=v_t} = r(t) \qquad \text{absorbing boundary at } v_t \tag{2.4}$$

$$\lim_{v\to-\infty} p(v,t) = 0 \qquad \text{natural boundary at } -\infty \tag{2.5}$$

$$\lim_{\Delta v\to 0} p(v_r + \Delta v, t) - p(v_r - \Delta v, t) = 0 \qquad \text{continuity at } v_r \tag{2.6}$$

$$\int_{-\infty}^{v_t} dv p(v,t) + \int_{t-\tau_{ref}}^{t} dt' r(t') = 1 \qquad \text{normalization} \tag{2.7}$$

The last term appearing in the FPE may also be modeled as another boundary condition at v_r

$$-D\partial_v p(v,t)|_{v=v_r} = r(t-\tau_{ref}). \tag{2.8}$$

We now want to investigate the influence of a weak input signal. Since we are interested in the second order response we may assume that the input signal is such that, besides the first order, we need to specify the second order in the Volterra series for the firing rate, which now reads

$$r(t) = r_0 + \int dt_1 h_1(t_1)s(t-t_1) + \int dt_1 \int dt_2 h_2(t_1,t_2)s(t-t_1)s(t-t_2). \tag{2.9}$$

To obtain the expressions for the susceptibilities we have to insert a specific signal $s(t)$ into this Volterra series in order to get an ansatz for the firing rate that we will insert into the FPE. Such a signal has to probe the whole frequency range of the system, so we choose the sum of two cosine functions [1, 2]

$$s(t) = \alpha\cos(\omega_1 t) + \beta\cos(\omega_2 t + \varphi). \tag{2.10}$$

Inserting the signal into the Volterra expansion of the firing rate (2.9) and using the definition of the susceptibilities (1.7) and (1.8) results in

$$\begin{aligned} r(t) = r_0 &+ \frac{\varepsilon}{2}\left(\alpha\chi_1(\omega_1)e^{-i\omega_1 t} + \beta\chi_1(\omega_2)e^{-i\omega_2 t}e^{-i\varphi} + c.c.\right) \\ &+ \frac{\varepsilon^2}{2}\left(\alpha^2\chi_2(\omega_1,-\omega_1) + \beta^2\chi_2(\omega_2,-\omega_2)\right) \\ &+ \frac{\varepsilon^2}{4}\left(\alpha^2\chi_2(\omega_1,\omega_1)e^{-i2\omega_1 t} + \beta^2\chi_2(\omega_2,\omega_2)e^{-i2\omega_2 t}e^{-i2\varphi} + c.c.\right) \\ &+ \frac{\varepsilon^2\alpha\beta}{2}\left(\chi_2(\omega_1,\omega_2)e^{-i(\omega_1+\omega_2)t}e^{-i\varphi} + \chi_2(\omega_1,-\omega_2)e^{-i(\omega_1-\omega_2)t}e^{i\varphi} + c.c.\right), \end{aligned} \tag{2.11}$$

where *c.c.* denotes the complex conjugate. We choose the above expression for the firing rate as an ansatz for solving the FPE and choose an analogous ansatz for the probability density

$$\begin{aligned} p(v,t) = p_0(v) &+ \frac{\varepsilon}{2}\left(\alpha p_1(v,\omega_1)e^{-i\omega_1 t} + \beta p_1(v,\omega_2)e^{-i\omega_2 t}e^{-i\varphi} + c.c.\right) \\ &+ \frac{\varepsilon^2}{2}\left(\alpha^2 p_2(v,\omega_1,-\omega_1) + \beta^2 p_2(v,\omega_2,-\omega_2)\right) \\ &+ \frac{\varepsilon^2}{4}\left(\alpha^2 p_2(v,\omega_1,\omega_1)e^{-i2\omega_1 t} + \beta^2 p_2(v,\omega_2,\omega_2)e^{-i2\omega_2 t}e^{-i2\varphi} + c.c.\right) \\ &+ \frac{\varepsilon^2\alpha\beta}{2}\left(p_2(v,\omega_1,\omega_2)e^{-i(\omega_1+\omega_2)t}e^{-i\varphi} + p_2(v,\omega_1,-\omega_2)e^{-i(\omega_1-\omega_2)t}e^{i\varphi} + c.c.\right). \end{aligned} \tag{2.12}$$

Inserting (2.11) and (2.12) into the FPE, we may sort out the terms in order of ε and stipulate that they all individually vanish. This results in the following hierarchy of equations

$$0 = \hat{L}_0 p_0(v) + r_0 \delta(v - v_r) \tag{2.13}$$

$$0 = (\hat{L}_0 + i\omega) p_1(v, \omega) - \partial_v p_0(v) + \chi_1(\omega) e^{i\omega\tau_{ref}} \delta(v - v_r) \tag{2.14}$$

$$\begin{aligned} 0 = &\left(\hat{L}_0 + i(\omega_1 + \omega_2)\right) p_2(v, \omega_1, \omega_2) + \chi_2(\omega_1, \omega_2) e^{i(\omega_1+\omega_2)\tau_{ref}} \delta(v - v_r) \\ &- \frac{1}{2} \left(\partial_v p_1(v, \omega_1) + \partial_v p_1(v, \omega_2)\right). \end{aligned} \tag{2.15}$$

Inserting the ansatz into the boundary conditions yields

$$p_{0,1,2}(v_t) = 0 \qquad \text{absorbing at } v_t \tag{2.16}$$

$$-D\partial_v p_k(v)|_{v=v_t} = \begin{cases} r_0, & k = 0 \\ \chi_k, & k = 1, 2 \end{cases} \qquad \text{absorbing at } v_t \tag{2.17}$$

$$\lim_{v \to -\infty} p_{0,1,2}(v) = 0 \qquad \text{natural at } -\infty \tag{2.18}$$

$$\lim_{\Delta v \to 0} p_{0,1,2}(v_r + \Delta v) - p_{0,1,2}(v_r - \Delta v) = 0 \qquad \text{continuity at } v_r \tag{2.19}$$

Let us note that the lower order probability densities appear as inhomogenities in the higher order equations, prompting us to solve the hierarchy from low to high.

2.2 Stationary case

In the stationary case we have to solve

$$0 = \hat{L}_0 p_0(v) + r_0 \delta(v - v_r) \tag{2.20}$$

We will follow the calculation performed in [19], which also introduces the notation $\hat{L}_0 = \partial_v(-f(v) + D\partial_v) = \partial_v(U'(v) + D\partial_v)$. The ordinary differential equation can be solved by using the method of variation of the constant – after employing all the boundary conditions the solution reads

$$p_0(v) = \frac{r_0}{D} e^{-\frac{U(v)}{D}} \int_v^{v_t} dv' e^{\frac{U(v')}{D}} \theta(v' - v_r). \tag{2.21}$$

There is one more unknown quantity, the stationary firing rate r_0 which has to be obtained via the normalization condition, resulting in

$$r_0 = D \left(\tau_{ref} D + \int_{v_r}^{v_t} dv_1 e^{\frac{U(v_1)}{D}} \int_{-\infty}^{v_1} dv_2 e^{-\frac{U(v_2)}{D}} \right)^{-1} \tag{2.22}$$

For certain potentials $U(v)$ the above expressions can be significantly simplified and result in known expressions, see table 2.1. However, it is worth stressing at this point that the above

formulae are closed solutions to the problem and even in cases where we can't further simplify the expressions they lend themselves to an easy numerical treatment.

	$U(v)$	r_0^{-1}
perfect	$-\mu v$	$\tau_{ref} + \frac{v_t - v_r}{\mu}$
leaky	$\frac{(v-\mu)^2}{2}$	$\tau_{ref} + \sqrt{\pi}\int_{\frac{\mu-v_r}{\sqrt{2D}}}^{\frac{\mu-v_t}{\sqrt{2D}}} dz e^{z^2}\mathrm{erfc}(z)$

Table 2.1: Stationary firing rate and probability density of the perfect and leaky integrate-and-fire models

2.3 Green's function and higher order equations

For the first order equation (2.14) we have to solve

$$0 = (\hat{L}_0 + i\omega)p_1(v,\omega) - \partial_v p_0(v) + \chi_1(\omega)e^{i\omega\tau_{ref}}\delta(v - v_r) \tag{2.23}$$

with the appropriate boundary conditions. We will solve it by using the Green's function formalism. Let us define the Green's function $G(v, v_r)$ via:

$$(\hat{L}_0 + i\omega)G(v, v_r) = -\delta(v - v_r), \tag{2.24}$$

where we have dropped the frequency argument for better readability. We may then find a general solution for our equation of the following form

$$\begin{aligned} p_1(v,\omega) &= \int_{-\infty}^{v_t} dv' G(v,v') \left(-\left[\partial_v p_0(v)\right]_{v=v'} + \chi_1(\omega)e^{i\omega\tau_{ref}}\delta(v' - v_r)\right) \\ &= G(v,v_r)\chi_1(\omega)e^{i\omega\tau_{ref}} - \int_{-\infty}^{v_t} dv' G(v,v')\left[\partial_v p_0(v)\right]_{v=v'} \end{aligned} \tag{2.25}$$

We will also apply this formalism to the second order equation (2.15), since it is of the same functional form as (2.14). The solution for the second order equation reads

$$\begin{aligned} p_2(v,\omega_1,\omega_2) = \int_{-\infty}^{v_t} dv' G(v,v') \Bigg(&-\frac{1}{2}\left[\partial_v p_1(v,\omega_1) + \partial_v p_1(v,\omega_2)\right]_{v=v'} \\ &+ \chi_2(\omega_1,\omega_2)e^{i(\omega_1+\omega_2)\tau_{ref}}\delta(v' - v_r)\Bigg) \\ = G(v,v_r)\chi_2(\omega_1,\omega_2)e^{i(\omega_1+\omega_2)\tau_{ref}} \\ - \frac{1}{2}\int_{-\infty}^{v_t} dv' G(v,v')\left[\partial_v p_1(v,\omega_1) + \partial_v p_1(v,\omega_2)\right]_{v=v'} \end{aligned} \tag{2.26}$$

It is now evident that we have to calculate the Green's function to obtain solutions for the probability densities. Let us procede to do so by introducing an auxiliary function $q(v, v_r)$ via

$$G(v, v_r) = \exp\left[-\frac{U(v) - U(v_r)}{2D}\right] q(v, v_r) := e_-(v) q(v, v_r), \tag{2.27}$$

which has to fulfill

$$\left[\frac{U''}{2} - \frac{(U')^2}{4D} + i\omega\right] q + Dq'' = -\delta(v - v_r). \tag{2.28}$$

We introduced this function to get rid of the first order derivative that would otherwise appear. We may exclude the δ-function by solving the equation in the domain left and right of v_r and state that the first derivative has a jump at v_r. Let us denote the solution for $v < v_r$ with $q_l(v)$ and the solution for $v > v_r$ with $q_r(v)$. All boundary conditions can then be summarized as

$$q_r(v_t) = 0 \tag{2.29}$$

$$\lim_{v \to -\infty} q_l(v) = 0 \tag{2.30}$$

$$q_l(v_r) = q_r(v_r) \tag{2.31}$$

$$q_r'(v_r) - q_l'(v_r) = -1/D \tag{2.32}$$

Generally, since this is an ordinary differential equation of second order, we have two independent solutions $q_1(v), q_2(v)$, so two parameters that have to be determined from the boundary conditions. Let us first of all note that due to Abel's identity we have

$$q_1(v) q_2'(v) - q_1'(v) q_2(v) = C := 1, \forall v, \tag{2.33}$$

where we set the appearing constant to 1, all other constants will then be scaled accordingly. We may also assume that one of these solutions shows the behavior $\lim_{v \to -\infty} q_1(v) = 0$. We then make the following ansatz for the solutions left and right of v_r

$$q_l(v) = C_1 q_1(v) + C_2 q_2(v) \tag{2.34}$$

$$q_r(v) = C_3 q_1(v) + C_4 q_2(v). \tag{2.35}$$

We exploit the boundary conditions to determine the free constants and put the left and right solution together so that our result is

$$q(v) = \frac{1}{D q_1(v_t)} \begin{cases} \left[q_2(v_t) q_1(v_r) - q_2(v_r) q_1(v_t)\right] q_1(v), & v < v_r \\ q_1(v_r) \left[q_2(v_t) q_1(v) - q_1(v_t) q_2(v)\right], & v > v_r \end{cases} \tag{2.36}$$

which results in a fully determined expression for our Green's function.

2.4 Expressions for the higher order susceptibilities

To obtain expressions for the higher order susceptibilities we have to evaluate the boundary condition at v_t

$$\chi_1(\omega) = -D\partial_v p_1(v,\omega)|_{v=v_t} \tag{2.37}$$
$$\chi_2(\omega_1,\omega_2) = -D\partial_v p_2(v,\omega_1,\omega_2)|_{v=v_t} \tag{2.38}$$

which, using that

$$\partial_v G(v,v_r)|_{v=v_t} = -\exp\left[-\frac{U(v_t)-U(v_r)}{2D}\right]\frac{q_1(v_r)}{Dq_1(v_t)} \tag{2.39}$$

results in

$$\chi_1(\omega) = -\frac{\int_{-\infty}^{v_t} dv p_0'(v)\exp\left[-\frac{U(v_t)-U(v)}{2D}\right]q_1(v)}{q_1(v_t) - e^{i\omega\tau_{ref}}\exp\left[-\frac{U(v_t)-U(v_r)}{2D}\right]q_1(v_r)} \tag{2.40}$$

$$\chi_2(\omega_1,\omega_2) = -\frac{1}{2}\frac{\int_{-\infty}^{v_t} dv\left(p_1'(v,\omega_1)+p_1'(v,\omega_2)\right)\exp\left[-\frac{U(v_t)-U(v)}{2D}\right]q_1(v,\omega_1+\omega_2)}{q_1(v_t,\omega_1+\omega_2) - e^{i\omega\tau_{ref}}\exp\left[-\frac{U(v_t)-U(v_r)}{2D}\right]q_1(v_r,\omega_1+\omega_2)}. \tag{2.41}$$

We stress at this point that the above expressions are closed form statements of the first and second order susceptibilities for a general integrate-and-fire neuron. They involve nested functions that can all be fundamentally reduced to knowing two functions: the potential $U(v)$ and the solutions $q_1(v), q_2(v)$ to the differential equation (2.42). All that is left to do in the specific case is to solve the differential equation

$$\left[\frac{U''}{2} - \frac{(U')^2}{4D} + i\omega\right]q + Dq'' = 0. \tag{2.42}$$

We show some analytical solutions in fig. 2.1. We note that for a general integrate-and-fire

$U(v)$	$q_1(v)$	$q_2(v)$
$-\mu v$	$\exp\left[v\sqrt{\frac{\mu^2}{4D^2}-\frac{i\omega}{D}}\right]$	$\exp\left[-v\sqrt{\frac{\mu^2}{4D^2}-\frac{i\omega}{D}}\right]$
$\frac{(v-\mu)^2}{2}$	$\mathcal{D}_{i\omega}\left(\frac{v-\mu}{\sqrt{D}}\right)$	$\mathcal{D}_{i\omega}\left(-\frac{v-\mu}{\sqrt{D}}\right)$

Figure 2.1: Analytical solutions to (2.42) for common integrate-and-fire models.

neuron the integrals in (2.40) and (2.41) can not be simplified further, generally prompting a numerical treatment. However, in the following we will show for the leaky integrate-and-fire neuron that the expressions can be simplified dramatically.

In the case of the leaky integrate-and-fire neuron we have $U(v) = \frac{(v-\mu)^2}{2}$ and the differential

equation (2.42) has the solutions

$$q_1(v) = \mathcal{D}_{i\omega}(\frac{v-\mu}{\sqrt{D}}) \tag{2.43}$$

$$q_2(v) = \mathcal{D}_{i\omega}(\frac{v-\mu}{\sqrt{D}}). \tag{2.44}$$

We introduce the function

$$f(v) = \exp\left[\frac{U(v)-U(v_t)}{2D}\right] q_1(v) = \exp\left[\frac{(v-\mu)^2-(v_t-\mu)^2}{2D}\right] D_{i\omega}\left(\frac{\mu-v}{D}\right), \tag{2.45}$$

which obeys the differential equation

$$Df'' + (v-\mu)f' + i\omega f = 0. \tag{2.46}$$

We can use this together with partial integration and the appropriate boundary conditions to simplify the integrals to

$$\int_{-\infty}^{v_t} dv p_0'(v) f(v) = \frac{r_0}{1-i\omega}\Big(f'(v_r,\omega) - f'(v_t,\omega)\Big) \tag{2.47}$$

and

$$\int_{-\infty}^{v_t} dv p_1'(v,\omega) f(v,\omega_1+\omega_2) = \frac{1}{1+i(\omega-\omega_1-\omega_2)}\left[\chi_1(\omega)\Big(f'(v_r,\omega_1+\omega_2)e^{i\omega_1\tau_r} - f'(v_t,\omega_1+\omega_2)\Big) + \frac{r_0}{2-i(\omega_1+\omega_2)}\Big(f''(v_r,\omega) - f''(v_t,\omega)\Big)\right]. \tag{2.48}$$

We may then utilize properties of the parabolic cylinder functions to simplify the derivatives of f

$$\partial_v f(v,\omega) = \exp\left[\frac{(v-\mu)^2-(v_t-\mu)^2}{2D}\right] D_{i\omega-1}\left(\frac{\mu-v}{D}\right)\frac{(-i\omega)}{\sqrt{D}} \tag{2.49}$$

$$\partial_v^2 f(v,\omega) = \exp\left[\frac{(v-\mu)^2-(v_t-\mu)^2}{2D}\right] D_{i\omega-2}\left(\frac{\mu-v}{D}\right)\frac{(-i\omega)(-i\omega-1)}{D} \tag{2.50}$$

to bring the results for the susceptibilities into their final form

$$\chi_1(\omega) = r_0 \frac{i\omega/\sqrt{D}}{i\omega - 1} \frac{\mathcal{D}_{i\omega-1}(\frac{\mu-v_t}{\sqrt{D}}) - e^{\Delta}\mathcal{D}_{i\omega-1}(\frac{\mu-v_r}{\sqrt{D}})}{\mathcal{D}_{i\omega}(\frac{\mu-v_t}{\sqrt{D}}) - e^{\Delta}e^{i\omega\tau_{ref}}\mathcal{D}_{i\omega}(\frac{\mu-v_r}{\sqrt{D}})} \tag{2.51}$$

$$\begin{aligned}\chi_2(\omega_1,\omega_2) = {} & r_0 \frac{(1-i\omega_1-i\omega_2)(i\omega_1+i\omega_2)}{2D(i\omega_1-1)(i\omega_2-1)} \frac{\mathcal{D}_{i\omega_1+i\omega_2-2}(\frac{\mu-v_t}{\sqrt{D}}) - e^{\Delta}\mathcal{D}_{i\omega_1+i\omega_2-2}(\frac{\mu-v_r}{\sqrt{D}})}{\mathcal{D}_{i\omega_1+i\omega_2}(\frac{\mu-v_t}{\sqrt{D}}) - e^{\Delta}e^{i(\omega_1+\omega_2)\tau_{ref}}\mathcal{D}_{i\omega_1+i\omega_2}(\frac{\mu-v_r}{\sqrt{D}})} \\ & + \frac{i\omega_1+i\omega_2}{2\sqrt{D}} \frac{\left(\frac{\chi_1(\omega_1)}{i\omega_2-1} + \frac{\chi_1(\omega_2)}{i\omega_1-1}\right)\mathcal{D}_{i\omega_1+i\omega_2-1}(\frac{\mu-v_t}{\sqrt{D}})}{\mathcal{D}_{i\omega_1+i\omega_2}(\frac{\mu-v_t}{\sqrt{D}}) - e^{\Delta}e^{i(\omega_1+\omega_2)\tau_{ref}}\mathcal{D}_{i\omega_1+i\omega_2}(\frac{\mu-v_r}{\sqrt{D}})} \\ & - \frac{i\omega_1+i\omega_2}{2\sqrt{D}} \frac{\left(\frac{\chi_1(\omega_1)e^{i\omega_1\tau_{ref}}}{i\omega_2-1} + \frac{\chi_1(\omega_2)e^{i\omega_2\tau_{ref}}}{i\omega_1-1}\right)e^{\Delta}\mathcal{D}_{i\omega_1+i\omega_2-1}(\frac{\mu-v_t}{\sqrt{D}})}{\mathcal{D}_{i\omega_1+i\omega_2}(\frac{\mu-v_t}{\sqrt{D}}) - e^{\Delta}e^{i(\omega_1+\omega_2)\tau_{ref}}\mathcal{D}_{i\omega_1+i\omega_2}(\frac{\mu-v_r}{\sqrt{D}})},\end{aligned} \tag{2.52}$$

where $\Delta = [v_r^2 + v_t^2 + 2\mu(v_t - v_r)]/(4D)$. The linear susceptibility is consistent with [20, 21] and the second order susceptibility was already obtained in [1, 2] through essentially the same calculation, however they consider the specific case of a leaky integrate-and-fire neuron, where we started from expressions for a general integrate-and-fire neuron.

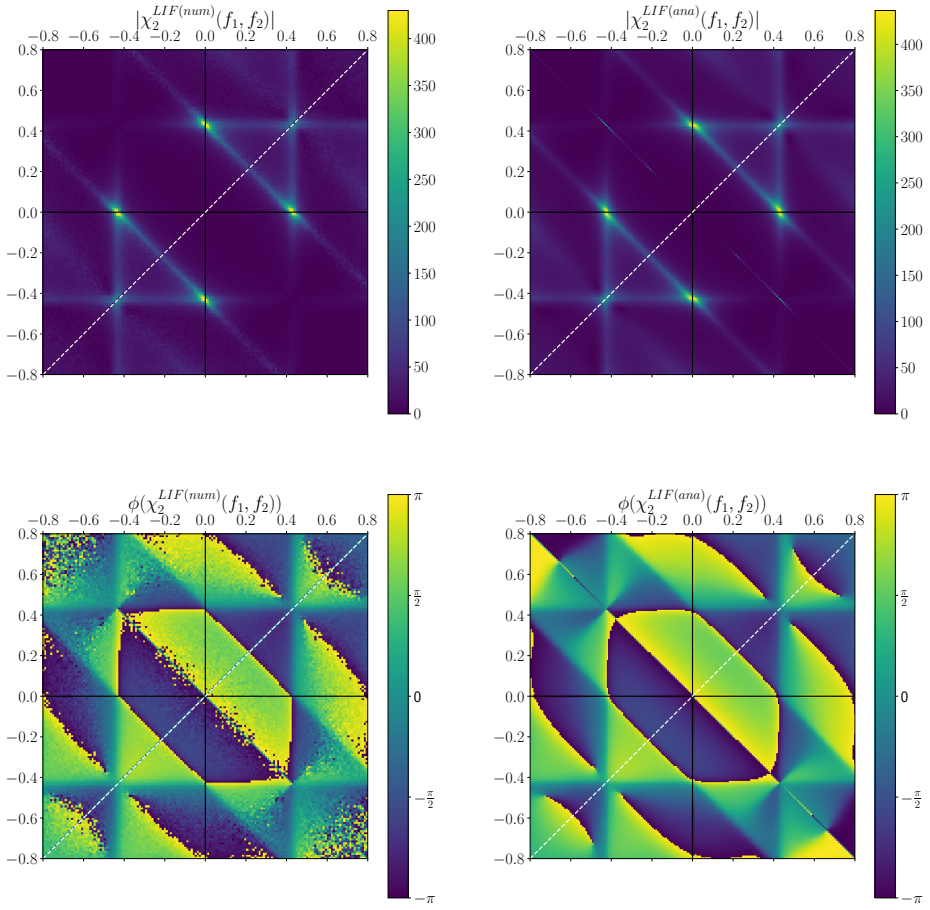

Figure 2.2: Second order susceptibility of the LIF. We show the absolute value (top row) and complex angle (bottom row) of the second order susceptibility of a leaky integrate-and-fire neuron (LIF). On the left side we show data that has been obtained using the measurement scheme presented in chapter 3 and on the right side we calculated the second order susceptibility using (2.52). Parameters: $\mu = 1.1, D = 10^{-3}, T = 100, \Delta t = 5 \cdot 10^{-3}, N = 10^5$.

CHAPTER 3

Measurement of higher order susceptibilities in integrate-and-fire models

To give a contrast to the analytic calculations in chapter 2 we will show how to numerically measure (higher order) susceptibilities for an integrate-and-fire model. The presented formalism may be used for all neuronic black box systems and will provide us with a numeric scheme with which we may show the fitness of our analytic solutions. Furthermore we will clarify the dependence of the susceptibilities on internal parameters such as the noise intensity.

3.1 Higher order susceptibilities are higher order spectra

In the last chapter we have seen how to analytically calculate the susceptibilities for general integrate-and-fire models. We now want to present a simulation scheme with which we can identify the susceptibilities, allowing us to compare our analytic predictions with numerical measurement. The central object of our scheme is a black box, as it is often used in the field of system identification. In our case the black box is a neuronic one, i.e. its time dependent input $s(t)$ will be some sort of electric signal and its time dependent output will be the spike train $x(t) = \sum_i \delta(t - t_i)$ with the spike times $\{t_i : i \in \mathbb{N}\}$. An advantage of considering such

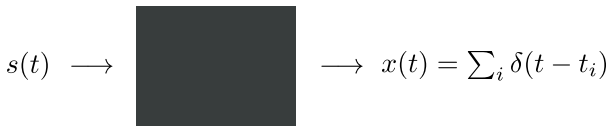

Figure 3.1: Neuron black box. We consider an unknown neuronic system that takes some time dependent input signal $s(t)$ and produces a spike train $x(t)$ with spike times t_i.

a neuronic black box is that we are not restricted to integrate-and-fire models with or without adaptation. We are striving for a measurement scheme where we can probe the whole frequency range of the susceptibilities. Evidently, this can not be achieved with a single cosine signal for example, because such a signal would only probe our system at a single frequency. A sum of cosine signals would be a more promising idea, but it would still only probe the system at a discrete set of frequencies. We therefore choose as our input signal $s(t)$ gaussian white noise with variance A

$$\langle s(t) \rangle = 0, \quad \langle s(t)s(t') \rangle = A\delta(t - t'), \tag{3.1}$$

which broadly excites all frequencies equally. The key to obtaining formulae for the susceptibilities is to investigate the input-output correlation statistics in Fourier space, namely the power- and cross spectra which we define as follows

$$\langle x(\omega_1)s^*(\omega_2)\rangle = 2\pi S_{xs}(\omega_1)\delta(\omega_1-\omega_2) \tag{3.2}$$
$$\langle x(\omega_1)s(\omega_2)\rangle = 2\pi S_{xs}(\omega_1)\delta(\omega_1+\omega_2) \tag{3.3}$$
$$\langle s(\omega_1)s^*(\omega_2)\rangle = 2\pi A\delta(\omega_1-\omega_2) \tag{3.4}$$
$$\langle s(\omega_1)s(\omega_2)\rangle = 2\pi A\delta(\omega_1+\omega_2) \tag{3.5}$$
$$\langle x(\omega_1)s^*(\omega_2)s^*(\omega_3)\rangle = 2\pi S_{xss}(\omega_2,\omega_3)\delta(\omega_1-\omega_2-\omega_3). \tag{3.6}$$

First, for the first order susceptibility, we take a look at the cross spectrum (3.2). The average in (3.2) considers the internal degress of freedom (which we will denote by a subscript ξ) as well as the degrees of freedom of the signal (denoted by a subscript s). The internal degrees of freedom correspond to the noise of the black box itself, whereas the degrees of freedom of the signal correspond to different realizations of a – potentially stochastic – input signal. Carrying out the average over all internal degrees of freedom (denoted by the subscript ξ) results in

$$\langle x(\omega_1)s^*(\omega_2)\rangle = \langle\langle x(\omega_1)s^*(\omega_2)\rangle_\xi\rangle_s = \langle r(\omega_1)s^*(\omega_2)\rangle_s. \tag{3.7}$$

Now we can insert the firing rate, where we choose the Wiener series up to second order (1.11), which yields (we drop the subscript s in the averaging brackets)

$$\begin{aligned}
\langle r(\omega_1)s^*(\omega_2)\rangle = \langle &\left[\left(2\pi r_0 - 2\pi A\int d\omega'\chi_2(\omega',-\omega')\right)\delta(\omega_1)+\chi_1(\omega_1)s(\omega_1)\right.\\
&\left.+\frac{1}{2\pi}\int d\omega'\chi_2(\omega_1-\omega',\omega')s(\omega_1-\omega')s(\omega')\right]s^*(\omega_2)\rangle\\
&= \left(2\pi r_0 - 2\pi A\int d\omega'\chi_2(\omega',-\omega')\right)\delta(\omega_1)\langle s^*(\omega_2)\rangle + \chi_1(\omega_1)\langle s(\omega_1)s^*(\omega_2)\rangle\\
&+\frac{1}{2\pi}\int d\omega'\chi_2(\omega_1-\omega',\omega')\langle s(\omega_1-\omega')s(\omega')s^*(\omega_1)\rangle\\
&= \chi_1(\omega_1)2\pi A\delta(\omega_1-\omega_2).
\end{aligned} \tag{3.8}$$

We have used the fact that all odd correlation functions of a gaussian signal vanish. By comparing (3.8) with the definition (3.2) we can identify

$$\chi_1(\omega) = \frac{S_{xs}(\omega)}{A}. \tag{3.9}$$

For the second order susceptibility we have to investigate the higher order cross spectrum (3.6). We again average over all internal degrees of freedom and insert the Wiener series for the firing

rate up to second order

$$\begin{aligned}\langle r(\omega_1)s^*(\omega_2)s^*(\omega_3)\rangle = \langle &\left[\left(2\pi r_0\delta(\omega_1) - 2\pi A\int d\omega\chi_2(\omega,-\omega)\right)\delta(\omega_1) + \chi_1(\omega_1)s(\omega_1)\right.\\ &\left.+\frac{1}{2\pi}\int d\omega\chi_2(\omega_1-\omega,\omega)s(\omega_1-\omega)s(\omega)\right]s^*(\omega_2)s^*(\omega_3)\rangle\\ &= \left(2\pi r_0\delta(\omega_1) - 2\pi A\int d\omega\chi_2(\omega,-\omega)\right)\delta(\omega_1)\langle s^*(\omega_2)s^*(\omega_3)\rangle\\ &+\chi_1(\omega_1)\langle s^*(\omega_1)s^*(\omega_2)s^*(\omega_3)\rangle\\ &+\frac{1}{2\pi}\int d\omega\chi_2(\omega_1-\omega,\omega)\langle s(\omega_1-\omega)s(\omega)s^*(\omega_2)s^*(\omega_3)\rangle. \end{aligned} \tag{3.10}$$

Again, the three point function vanishes and we can simplify the four point function as follows

$$\begin{aligned}\langle s(\omega_1-\omega)s(\omega)s^*(\omega_2)s^*(\omega_3)\rangle &= \langle s(\omega_1-\omega)s(\omega)\rangle\langle s^*(\omega_2)s^*(\omega_3)\rangle\\ &+\langle s(\omega_1-\omega)s^*(\omega_2)\rangle\langle s(\omega)s^*(\omega_3)\rangle\\ &+\langle s(\omega_1-\omega)s^*(\omega_3)\rangle\langle s(\omega)s^*(\omega_2)\rangle\\ &= 4\pi^2A^2\left[\delta(\omega_1)\delta(\omega_2+\omega_3)+\delta(\omega_1-\omega-\omega_2)\delta(\omega-\omega_3)\right.\\ &\left.+\delta(\omega_1-\omega-\omega_3)\delta(\omega-\omega_2)\right]. \end{aligned} \tag{3.11}$$

The cross spectrum then reads

$$\langle x(\omega_1)s^*(\omega_2)s^*(\omega_3)\rangle = 2\pi\delta(\omega_1-\omega_2-\omega_3)\left(r_0A\delta(\omega_2+\omega_3)+2A^2\chi_2(\omega_2,\omega_3)\right), \tag{3.12}$$

which, after rearranging, yields the following expression for the second order susceptibility

$$\chi_2(\omega_1,\omega_2) = \frac{S_{xss}(\omega_1,\omega_2)}{2A^2} - \frac{r_0}{2A}\delta(\omega_1+\omega_2). \tag{3.13}$$

The delta function in this expression seems kind of troublesome, but we can explain its origin. It comes about the same way as the delta function in (1.11) – due to a nonzero average before Fourier transforming. The two expressions (3.9) and (3.13) have already been obtained using a different calculation by [22] for a general black box system. They consider the Fourier transform of the Lee-Schetzen-formulae, reaching the same result as we have.

Both expressions lend themselves to a simple numerical treatment. In a simulation one performs the steps shown in fig. 3.2. For more detailed numerical insights see chapter 5. The presented procedure of inserting a higher order Wiener series for the firing rate into a higher order cross spectrum can be advanced further to yield the third, fourth (and so on) order susceptibilities. We have to stress at this point, that the obtained quantities are *Wiener* susceptibilities. To obtain the corresponding Volterra susceptibilities, one has to use the Wiener-to-Volterra formulae presented in chapter 1.

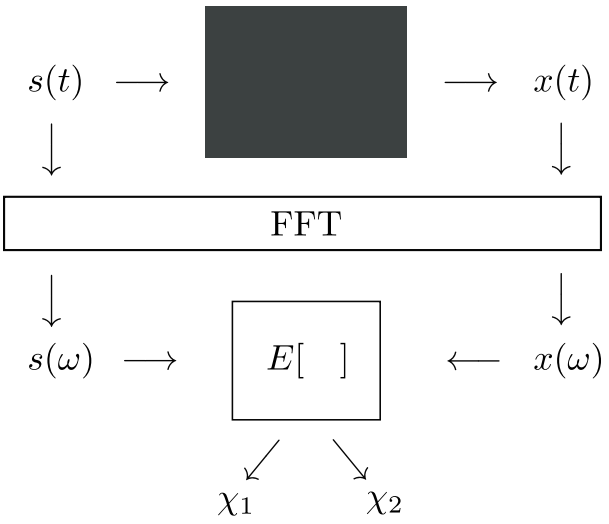

Figure 3.2: Simulation scheme. We generate a gaussian white noise input signal $s(t)$ with variance A. Then we record the output $x(t)$. We use a fast Fourier transform (FFT) to obtain $s(\omega)$ and $x(\omega)$. Then we use (3.9) and (3.13) to obtain the susceptibilities.

3.2 Parameter dependence of first order susceptibilities

This section closely follows a calculation performed in [19]. In the last section we derived formulae for the measurement of the susceptibilities, where we always explicitly denoted their frequency dependence, $\chi_1(\omega), \chi_2(\omega_1, \omega_2)$. They, however, do not only depend on the frequency, but also on the internal parameters of the system – in the case of integrate-and-fire models the internal parameters are the mean input current μ and the noise intensity D. If we now apply a white noise signal as proposed in the last section, this begs the following question: Do the susceptibilities depend only on the internal noise strength or do they depend on the sum of input noise and internal noise strength? To answer this question let us investigate a general integrate-and-fire neuron of the following form

$$\dot{v} = f(v;\mu) + \underbrace{\sqrt{2Dc}\xi_s(t)}_{\text{signal}} + \underbrace{\sqrt{2D(1-c)}\xi_n(t)}_{\text{noise}} \tag{3.14}$$

with the usual fire-and-reset rule $v > v_t \to v = v_r$. The total noise has the intensity $2D$ and is split into a signal part (denoted with the subscript s) and an intrinsic noise part (denoted with the subscript n). Both the signal and the intrinsic noise are white and gaussian with variance one. At this point we might say that we can simply add the signal and the intrinsic noise together, but then what is the small external signal we need for our perturbation calculation?

Let us now split up the signal noise into N independent noise processes $\eta_i(t)$ which all have unit variance just as ξ_s

$$\sqrt{2Dc}\xi_s(t) = \sqrt{\frac{2Dc}{N}} \sum_{i=1}^{N} \eta_i(t), \tag{3.15}$$

where we scale by a factor of $1/\sqrt{N}$ because the variances of these gaussian processes add up. We now single out one of these independent noise processes to be our weak signal (answering our question from before) and regard the rest of them as an additional contribution to the background noise. Here, we have arbitrarily chosen the first noise process η_1 to be the weak signal. In the limit of infinitely many subprocesses the total (intrinsic) noise is then given by

$$\text{intrinsic noise} = \sqrt{2D(1-c)}\xi_n(t) + \sqrt{\frac{2Dc}{N}}\sum_{i=2}^{N}\eta_i(t) \overset{N\to\infty}{\to} \sqrt{2D}\xi(t). \tag{3.16}$$

The input-output correlation of our spike train with the noise signal is

$$\langle x(\omega_1)\sqrt{2Dc}\xi_s^*(\omega_2)\rangle = \sum_{i=1}^{N}\langle x(\omega_1)\sqrt{\frac{2Dc}{N}}\eta_i^*(\omega_2)\rangle = N\langle x(\omega_1)\sqrt{\frac{2Dc}{N}}\eta_1^*(\omega_2)\rangle \tag{3.17}$$

because all the subprocesses share the same correlation with the output. This correlation is now given by

$$\langle x(\omega_1)\sqrt{\frac{2Dc}{N}}\eta_1^*(\omega_2)\rangle = \chi_1(\omega;\mu,D)2\pi\frac{2Dc}{N}\delta(\omega_1-\omega_2). \tag{3.18}$$

Therefore we can now finally conclude for the cross-spectrum

$$\begin{aligned} 2\pi S_{xs}(\omega)\delta(\omega_1-\omega_2) &= \langle x(\omega_1)s^*(\omega_2)\rangle \\ &= \langle x(\omega_1)\sqrt{2Dc}\xi_s^*(\omega_2)\rangle \\ &= 4\pi Dc\chi_1(\omega;\mu,D)\delta(\omega_1-\omega_2), \end{aligned} \tag{3.19}$$

yielding

$$\chi_1(\omega;\mu,D) = \frac{S_{xs}(\omega)}{2Dc}. \tag{3.20}$$

Comparing this to (3.9) we can see that the variance of the signal is $2Dc$, which is of course true. The most important point is that in the limit of infinitely many subprocesses all noise is intrinsic and that its strength (i.e. its variance) is given by $2D$, therefore the parametric dependence of the susceptiblity is $\chi_1(\omega;\mu,D)$ and *not* $\chi_1(\omega;\mu,D(1-c))$. To summarize, the susceptibility depends parametrically on the sum of both the intrinsic noise and the noise that serves as our input signal.

The noise split parameter c may be interpreted as a dial with which we adjust the signal-to-noise ratio. This is well illustrated in fig. 3.3. We can see that in all cases the numerically obtained data (colored lines) fluctuates around the analytic solution (black line). This is mainly due to the fact that we compute $\chi_1(f)$ using a finite number of trials – here we have chosen $N = 10^4$. By increasing the number of trials we could decrease these fluctuations. However, we can also see another effect in the plot – if we increase the noise split coefficient c, the fluctuations are reduced. By increasing the noise split coefficient c we are increasing the strength of the input signal and we are decreasing the strength of the internal noise, so we are maximizing our

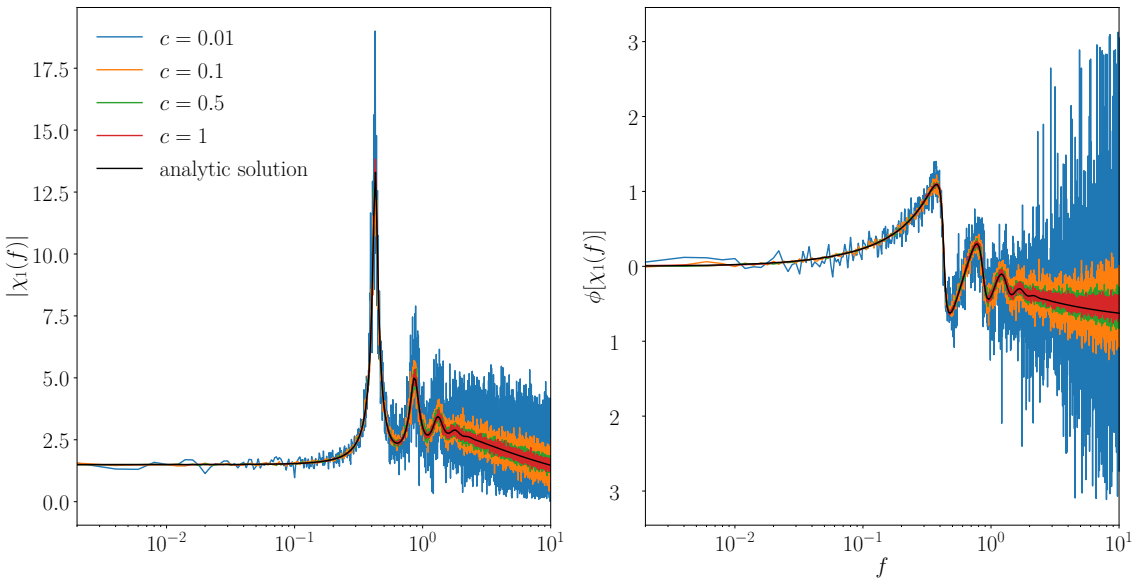

Figure 3.3: First order susceptibility of the LIF for different noise intensities. We consider a leaky integrate-and-fire neuron subject to white noise with the intensity Dc. The neuron has intrinsic noise intensity $D(1-c)$. Left panel: Absolute value of $\chi^{\mathrm{LIF}}(f;\mu,D)$. Right panel: Angle. The coloured lines present data from a simulation, the black line corresponds to the theory in (2.51). Parameters: $\mu = 1.1, D = 10^{-3}, T = 500, \Delta t = 10^{-3}, N = 10^4$.

signal-to-noise ratio. The optimal case $c = 1$, where we have no internal noise and the input signal was strength $2D$ gives us the most precise measurement of the susceptibility.

Coming back to the argument of the parametric dependency of the susceptibility we can see in fig. 3.3 that no matter the value of c, all curves are of the same form, because the susceptibility $\chi_1(f;\mu,D)$ depends on the sum of input and instrinsic noise intensity $Dc + D(1-c) = D$.

3.3 Parameter dependence of higher order susceptibilities

The same line of arguments as presented in the last section can be repeated for all higher order susceptibilities. To illustrate this let us take a look at the second order susceptibility. We consider the exact same setup as in the previous section, with the total noise split into intrinsic and signal noise by the noise split coefficient c. We also consider that the signal noise is split into N independent noise processes. The higher order cross spectrum then reads

$$\begin{aligned}\langle x(\omega_1)\sqrt{2Dc}\xi_s^*(\omega_2)\sqrt{2Dc}\xi_s^*(\omega_3)\rangle &= \sum_{i=1}^{N}\sum_{j=1}^{N}\langle x(\omega_1)\sqrt{\frac{2Dc}{N}}\eta_i^*(\omega_2)\sqrt{\frac{2Dc}{N}}\eta_j^*(\omega_3)\rangle \\ &= N^2\langle x(\omega_1)\sqrt{\frac{2Dc}{N}}\eta_1^*(\omega_2)\sqrt{\frac{2Dc}{N}}\eta_1^*(\omega_3)\rangle, \end{aligned} \tag{3.21}$$

because all η_i share the same correlation function. Again, in the limit of $N \to \infty$ the intrinsic noise strength is $2D$ and we know that

$$\langle x(\omega_1)\sqrt{\frac{2Dc}{N}}\eta_1^*(\omega_2)\sqrt{\frac{2Dc}{N}}\eta_1^*(\omega_3)\rangle = 2\pi\delta(\omega_1-\omega_2-\omega_3)\left(r_0\frac{2Dc}{N}\delta(\omega_2+\omega_3)\right.$$
$$\left.+2\left(\frac{2Dc}{N}\right)^2\chi_2(\omega_2,\omega_3;\mu,D)\right). \tag{3.22}$$

The higher order cross spectrum is then given by (we assume that $\omega_2 \neq -\omega_3$)

$$\begin{aligned}2\pi S_{xss}(\omega_2,\omega_3)\delta(\omega_1-\omega_2-\omega_3) &= \langle x(\omega_1)s^*(\omega_2)s^*(\omega_3)\rangle \\ &= \langle x(\omega_1)\sqrt{2Dc}\xi_s^*(\omega_2)\sqrt{2Dc}\xi_s^*(\omega_3)\rangle \\ &= 2\pi\delta(\omega_1-\omega_2-\omega_3)2(2Dc)^2\chi_2(\omega_2,\omega_3;\mu,D).\end{aligned} \tag{3.23}$$

We can rearrange this again to give us a familiar form for the second order susceptibility

$$\chi_2(\omega_1,\omega_2;\mu,D) = \frac{S_{xss}(\omega_1,\omega_2)}{2(2Dc)^2} \tag{3.24}$$

Just like the first order susceptibility, the second order susceptibility depends on the sum of intrinsic and signal noise strength.

It is clear that our line of reasoning may be readily applied to all higher order susceptibilities. The key argument is the separation of the input noise signal into N independent and identical subprocesses, where one of them serves as the weak input signal and then take the limit $N \to \infty$.

CHAPTER 4

Susceptibilities of the adapting leaky integrate-and-fire model

We calculate the susceptibilities for the leaky integrate-and-fire model with an adaptation current (LIFAC) and compare to the model without adaptation. In the first part we present an outline similar to [13], where the perfect integrate-and-fire model with an adaptation current has been presented. Towards the end of the chapter we will present approximations to the second order susceptibility of the LIFAC and compare it to the known result for the leaky integrate-and-fire model without adaptation [1, 2].

4.1 Adapting leaky integrate-and-fire model

There are two ways implementing the adaptation in the leaky integrate-and-fire model. The first is to consider a dynamic threshold where, everytime the neuron spikes, the threshold is increased. In the rest state the threshold then decays to a fixed value. The second way is to consider an adaptive current that jumps by a set amount everytime the neuron fires and then, again, decays to a fixed value. With respect to the spike frequency adaptation these two models can be regarded as equivalent [23], see also [24] where they show a transformation from one approach to the other. The leaky integrate-and-fire model with an adaptation current (in the following we will abbreviate it by LIFAC in accordance with [23, 25]) and an external signal is given by the following equations

$$\tau_m \dot{v} = \mu - v - a + s(t) + \sqrt{2D}\xi(t), \tag{4.1}$$

$$\tau_a \dot{a} = -a, \tag{4.2}$$

where $v(t)$ is the membrane voltage, $a(t)$ is the adaptation current, μ is the mean input current, $s(t)$ is a (potentially weak) input current and D is the noise coefficient. The two dynamics are associated with time scales given by the membrane time constant τ_m and the adaptation time constant τ_a. We impose a fire-and-reset rule: if $v > v_t \to v = v_r$ and $a \to a + \Delta$, where the latter may also be included in the dynamics

$$\tau_a \dot{a} = -a + \Delta \tau_a x(t), \tag{4.3}$$

where $x(t) = \sum_i \delta(t - t_i)$ is the spike train. It is useful to introduce dimensionless units by rescaling the time by the membrane time constant $t \to t/\tau$ and the voltage by the difference of the threshold and reset value $v \to (v - v_r)/(v_t - v_r)$ [26]. All parameters are taken care of

accordingly so that the dynamics now read

$$\dot{v} = \mu - v - a + s(t) + \sqrt{2D}\xi(t), \tag{4.4}$$

$$\tau_a \dot{a} = -a + \Delta\tau_a \sum_i \delta(t - t_i). \tag{4.5}$$

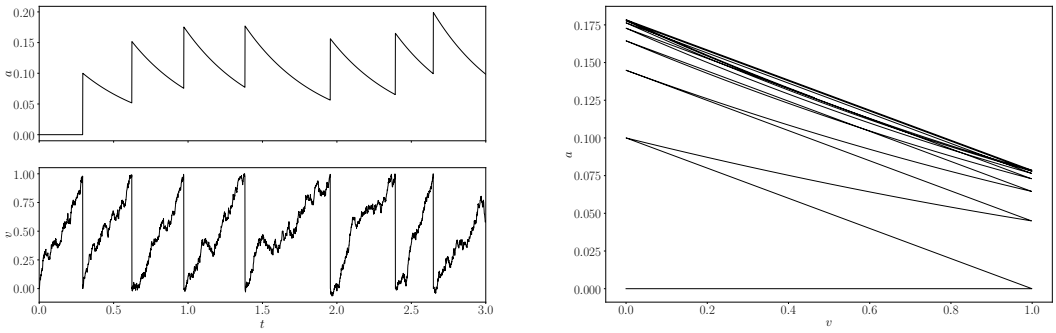

(a) (b)

Figure 4.1: Phase space of the LIFAC. (a): Trajectories of the leaky integrate-and-fire neuron with an adaptation current (LIFAC). Here we can clearly see the fire-and-reset rule: whenever v reaches the threshold $v_t = 1$, then it is reset to $v_r = 0$ and the adaptation jumps by Δ. The adaptation variable then decays exponentially until the next spike. (b): In the phase space $v - a$ the can see a limit cycle emerging for the case of no noise ($D = 0$). The diagonal lines from the lower right to upper left represent the reset rule. Parameter values: $\mu = 3.1, D = 0.1, \tau_a = 0.5, \Delta = 0.1, T = 3.0, \Delta t = 10^{-3}$.

As a first observation we note that the dynamics of the adaptation variable can be solved exactly

$$a(t) = \sum_i \Delta e^{\frac{t-t_i}{\tau_a}} \Theta(t - t_i), \tag{4.6}$$

so it is a sum of exponenial functions that decay with the decay time τ_a between two spikes. The Heaviside function simply expresses the notion that a spike may only influence subsequent spikes.

In the nonadapting leaky integrate-and-fire model the system loses all memory between spikes through the fire-and-reset mechanism. The adaptation variable allows us to introduce correlations between spike times. More specifically the adaptation negatively correlates the spikes, which means that short interspike intervals will – more likely – be followed by a long interspike interval.

4.2 Slow adaptation, stationary case

Let us consider the case where $\tau_a \gg \langle T \rangle$, i.e. the adaptation is much slower than the mean firing of the neuron. In this limit the relative deviations of $a(t)$ about its mean value are small and we can replace $a(t)$ with its mean value $\langle a \rangle$. Averaging the differential equation for the adaptation value gives us a connection between the stationary firing rate and the mean value of the adaptation variable

$$\langle a \rangle = \Delta \tau_a r_0(\hat{\mu}, D). \tag{4.7}$$

In the slow adaptation approximation our model is reduced to a nonadapting leaky integrate-and-fire neuron with the reduced mean input current $\hat{\mu} = \mu - \langle a \rangle$. Its firing rate may then be determined via

$$r_0(\hat{\mu}, D) = \left(\sqrt{\pi} \int_{\frac{\hat{\mu}-v_t}{\sqrt{2D}}}^{\frac{\hat{\mu}-v_r}{\sqrt{2D}}} dz \; e^{z^2} \mathrm{erfc}(z) \right)^{-1}. \tag{4.8}$$

This equation together with (4.7) has to be solved self consistently, which can not be done analytically. However, the solution may be found numerically in the following manner; we insert (4.7) into (4.8), which reads

$$\frac{\langle a \rangle}{\Delta \tau_a} = \left(\sqrt{\pi} \int_{\frac{\hat{\mu}-v_t}{\sqrt{2D}}}^{\frac{\hat{\mu}-v_r}{\sqrt{2D}}} dz \; e^{z^2} \mathrm{erfc}(z) \right)^{-1}. \tag{4.9}$$

From this equation we find, for a fixed set of parameters $(\mu, D, v_t, v_r; \Delta, \tau_a)$, a value for $\langle a \rangle$ by using a root finding algorithm (e.g. the bisection algorithm). We then insert this value back into the first equation to find r_0. Results for this approach are shown in fig. 4.2. It works generally well if we are in the limit of slow and weak adaptation, for stronger adaptation – i.e. either the time scale of the adaptation is short or the kick size is large – this semianalytic scheme fails.

There is, however, a limit in which we can make further analytical progress. In the mean-driven regime, i.e. $|\frac{\mu - v_{t,r}}{\sqrt{2D}}| \gg 1$ the firing rate is given by

$$r_0 = \left(\ln\left(\frac{\mu - v_r}{\mu - v_t} \right) - \frac{D}{2} \left(\frac{1}{(\mu - v_t)^2} - \frac{1}{(\mu - v_r)^2} \right) \right)^{-1}, \tag{4.10}$$

which if $\mu \gg v_t$ can be further simplified to

$$r_0 \overset{\mu \gg v_t}{\approx} \mu - \frac{1}{2} + \mathcal{O}(\mu^{-1}). \tag{4.11}$$

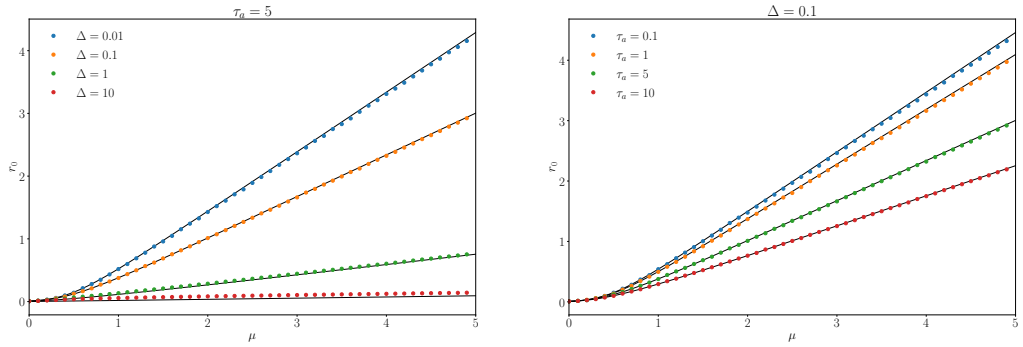

(a) (b)

Figure 4.2: Firing rate of the LIFAC. We compare the approach of using the self consistency equation (4.9) (solid black lines) to calculate the stationary firing rate to a simulation (colored points). We conclude that increasing either value τ_a or Δ decreases the firing rate. (a): Fixed τ_a several values of Δ. (b): Fixed Δ and several values of τ_a. Parameter values: $D = 0.1, T = 10^4, \Delta t = 10^{-3}$.

Therefore, in the strongly mean driven regime, we have

$$r_0 = \frac{1}{1 + \Delta\tau_a}\left(\mu - \frac{1}{2}\right) \tag{4.12}$$

the firing rate depends linearly on the mean input current and the slope is dependent on the product $\Delta\tau_a$.

4.3 Slow adaptation, response to stimuli

Let us now consider the case where our model is also subject to an external, time dependent signal. In this case the firing rate will also vary as time passes and through the feedback mechanism, the adaptation variable will also change over time. We want to employ response theory which usually stipulates that the perturbations are small in some sense. Let us rewrite our dynamics as follows

$$\dot{v} = \underbrace{\mu - \langle a \rangle}_{:=\hat{\mu}} - v \underbrace{- \big(a - \langle a \rangle\big) + s(t)}_{\text{perturbation}} + \sqrt{2D}\xi(t), \tag{4.13}$$

where now the perturbation is the external signal *and* the variance of the adaptation around its mean value. Notice, that our rewrite results in a *reduced mean input current* $\hat{\mu}$. While we may stipulate that the external signal is weak, the case for the adaptation is not so easy. First of all, we mean value of the adaptation is still time dependet, as can be seen by considering

the average of (4.6)

$$\langle a\rangle(t) = \Delta \int_0^t ds e^{\frac{t-s}{\tau_a}} r(s). \tag{4.14}$$

We now assume that the mean adaptation does not vary a lot around its time independent mean, which we can calculate by replacing $r(s) \to r_0$ in the integral, leaving $\langle a\rangle = \Delta\tau_a r_0$. The "smallness" of the perturbation of the adaptation is now determined by the magnitude of the term $(a - \langle a\rangle)$. In Ref. [13] the magnitude of the fluctuations of the adaptation variable are quantified and we will repeat the arguments here. Consider the Fourier transform of the adaptation current (this can easily be calculated by Fourier transforming the equation for $a(t)$)

$$a(\omega) = \frac{\Delta\tau_a}{1 - i\tau_a\omega} x(\omega), \tag{4.15}$$

where $x(\omega)$ is the Fourier transform of the spike train. We may then express the power spectrum of the adaptation variable through the power spectrum of the spike train

$$S_{aa}(\omega) = \frac{\Delta^2\tau_a^2}{1 + \tau_a^2\omega^2} S_{xx}(\omega). \tag{4.16}$$

The power spectrum is related to the variance of a zero mean process like so

$$\langle \Delta a^2\rangle = \sigma^2 = \int \frac{d\omega}{2\pi} S_{aa}(\omega) \tag{4.17}$$

In the slow adaptation limit ($\tau_a \to \infty$) we only consider vanishingly small frequencies under the integral. Knowing that the power spectrum of the spike train saturates at a finite value for $\omega \to 0$ we can write

$$\langle \Delta a^2\rangle = \int \frac{d\omega}{2\pi} \frac{\Delta^2\tau_a^2}{1 + \tau_a^2\omega^2} S_{xx}(\omega) \propto \Delta^2\tau_a. \tag{4.18}$$

Now comes a tricky point. Ref. [13] uses a different parametrization for the adaptation, instead of the kick size Δ they consider a rescaled kicksize $\tilde{\Delta} = \Delta\tau_a$. They then state that for a fixed $\tilde{\Delta}$ the variance of the adaptation variable vanishes for $\tau_a \to \infty$. We have to slightly modify this statement to the following: the variance of the adaptation variable vanishes in the limit of slow adaptation *and* if $\Delta^2\tau_a \to 0$, so the kick size also has to get smaller. To summarize, for the perturbation caused by the adaptation in (4.13) to be small we stipulate that the adaptation time τ_a is significantly longer than the intrinsic time scale, given by the mean interspike interval $\langle T\rangle = 1/r_0$ and that the kick size of the adaptation Δ is small.

We now want to employ the Volterra series and expand the firing rate up to second order in the signal [1]

$$r(t) = r_0 + \int dt_1 h(t_1) s(t - t_1) + \int dt_1 \int dt_2 h_2(t_1, t_2) s(t - t_1) s(t - t_2) \tag{4.19}$$

Since we want to obtain expressions for the susceptibilities we will work with the Fourier

transform, which reads

$$r(\omega) = 2\pi r_0 \delta(\omega) + \chi_1(\omega)s(\omega) + \frac{1}{2\pi}\int d\omega_1 \chi_2(\omega_1, \omega - \omega_1)s(\omega_1)s(\omega - \omega_1) \tag{4.20}$$

We thereby assume that the perturbation is weak enough, so that we can neglect even higher orders and strong enough so that a description using only the linear order does not suffice. The Volterra series considers a general perturbation, for our case we have to insert the sum of adaptation and the weak input signal

$$s(t) \to s(t) - a(t) + \langle a \rangle, \tag{4.21}$$

$$s(\omega) \to s(\omega) - \frac{\Delta\tau_a}{1 - i\tau_a\omega}x(\omega) + 2\pi\langle a\rangle\delta(\omega). \tag{4.22}$$

Note also that (4.20) differs from (1.11) only by the static term.

4.3.1 First order susceptibility

Let us first take a step back and only consider the Volterra expansion up to first order

$$r(\omega) = 2\pi r_0 \delta(\omega) + \chi_1(\omega; \hat{\mu}, D)\left(s(\omega) - \frac{\Delta\tau_a}{1 - i\tau_a\omega}x(\omega) + 2\pi\langle a\rangle\delta(\omega)\right). \tag{4.23}$$

This statement is somewhat problematic since on the left side we have the average over all realizations of the spike train, i.e. the firing rate, whereas on the right side the spike train explicitly appears. Ref. [13] deals with this problem by stating that if the feedback provided by the adaptation is weak, then this perturbation must be self consistently solved by considering its average. Ref. [27] resolves the issue by considering the spike train also on the left side of (4.23), which is an ansatz similar to the linear-fluctuation approximation. We will proceed by carrying out the average on the right side of the equation so we can rearrange for the firing rate

$$r(\omega) = 2\pi\delta(\omega)r_0 + \frac{\chi_1(\omega; \hat{\mu}, D)}{1 + \chi_1(\omega; \hat{\mu}, D)\frac{\Delta\tau_a}{1 - i\tau_a\omega}}s(\omega). \tag{4.24}$$

We can now identify the first order susceptibility by comparing to the Volterra expansion of first order

$$\chi_1^{\mathrm{LIFAC}}(\omega; \mu, D, \tau_a, \Delta) = \left(\frac{1}{\chi_1^{\mathrm{LIF}}(\omega; \hat{\mu}, D)} + \frac{\Delta\tau_a}{1 - i\tau_a\omega}\right)^{-1}. \tag{4.25}$$

This first order susceptibility is algebraically identical to the case of a perfect integrate-and-fire neuron investigated in [13]. From now on we will drop the parametric dependencies of the susceptibilities, but we note that the susceptibility for the LIFAC involves the susceptibility for the LIF with the *reduced* mean input current. In Fig. fig. 4.3 we show a comparison of this formula to a numerical measurement of the first order susceptibility, where we have chosen the kick size to be small. As a comparison we have also plotted the theory for a nonadapting leaky

integrate-and-fire neuron with the reduced mean input current $\hat{\mu}$ as a dashed line. We can see that (4.25) describes the data well, even for the case that the adaptation time constant τ_a is in the range of the mean interspike interval $\langle T \rangle$. The main difference between the susceptibility for the LIFAC and the LIF with a reduced base current occurs for small frequencies, where the transition takes place at $\omega \approx 1/\tau_a$. For small frequencies the suppression in the absolute value

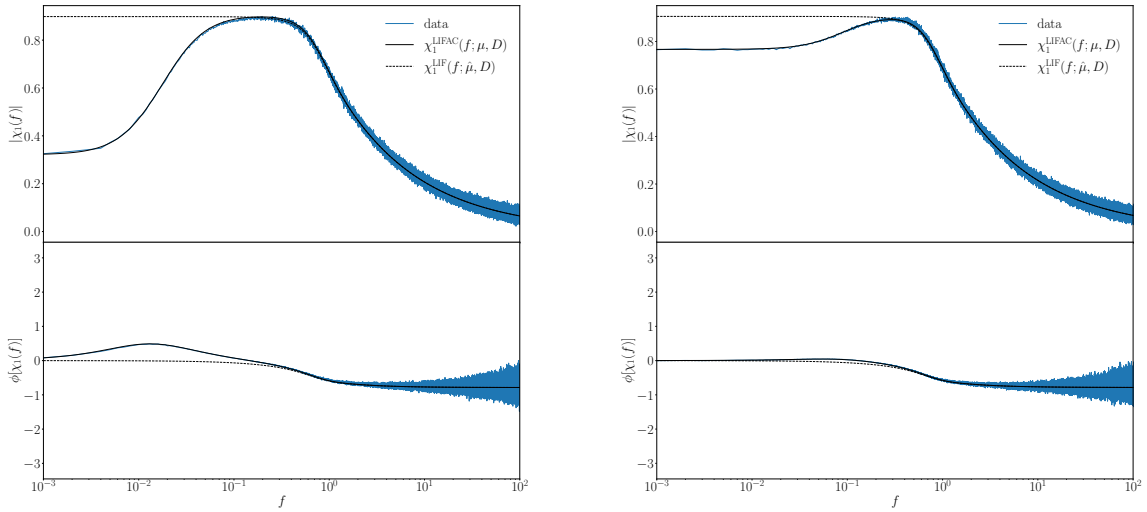

Figure 4.3: First order susceptibility of the LIFAC: Upper panels show the absolute value, lower panels the complex angle of the first order susceptibility. The blue lines represent data obtained from a simulation (see chapter 5), the solid black lines are the theory given in (4.25), the dashed black lines represent the theory for a nonadapting leaky integrate-and-fire neuron with the reduced mean input current $\hat{\mu}$. In both plots we have chosen a small kick size of the adaptation, in (a) the time constant of the adaptation is large $\tau_a \gg \langle T \rangle$, in (b) it is comparable to the mean interspike interval $\tau_a \approx \langle T \rangle$.
Parameters for (a): $\mu = 2.0, \tau_a = 20.0$, resulting in $\langle T \rangle \approx 1.94$. Parameters for (b): $\mu = 1.1, \tau_a = 2.0$, resulting in $\langle T \rangle \approx 1.85$. Parameters for both plots: $T = 10^3, \Delta t = 5 \cdot 10^{-4}, N = 10^4, D = 0.1, \Delta = 0.1$.

of the first order susceptibility is given by

$$\chi_1^{\mathrm{LIFAC}}(\omega \to 0) = \frac{\chi_1^{\mathrm{LIF}}(\omega \to 0)}{1 + \Delta\tau_a \chi_1^{\mathrm{LIF}}(\omega \to 0)}, \tag{4.26}$$

so the absolute value of the susceptibility will be reduced (compared to the LIF case) due to the factor $|1/(1+\Delta\tau_a\chi_1^{\mathrm{LIF}})|$. In the limit of large frequencies the additional adaptation contribution vanishes, i.e. $\frac{\Delta\tau_a}{1-i\tau_a\omega} \to 0$, so that we have

$$\chi_1^{\mathrm{LIFAC}}(\omega \to \infty) = \chi_1^{\mathrm{LIF}}(\omega \to \infty) \tag{4.27}$$

The adaptation therefore works as a high-pass filter, suppressing lower frequencies while leaving higher frequencies unaltered. This behaviour is consistent with the findings for the adapting PIF model [13] and adapting neurons in general [28]. In fig. 4.4 we show a comparison of our

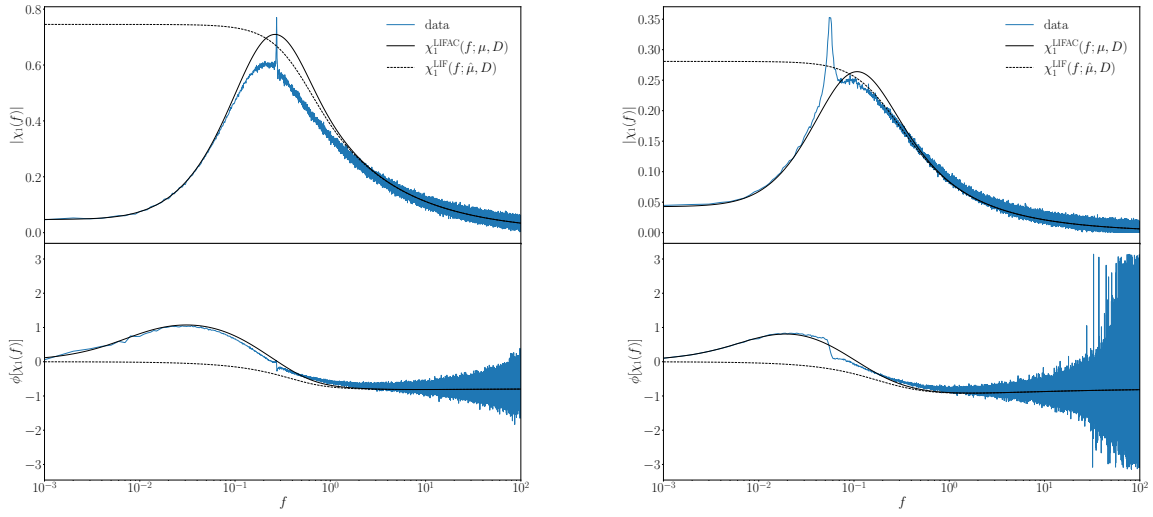

Figure 4.4: Same as fig. 4.3. However, in these plots we have chosen a large kick size of the adaptation. This leads to artifacts that are no longer described by our theory, such as a peak at the firing rate ($r_0 \approx 0.27$) in (a) and a peak at $1/\tau_a = 0.05$ in (b).
Parameters for (a): $\mu = 6.0, \tau_a = 20.0$, resulting in $\langle T \rangle \approx 3.75$. Parameters for (b): $\mu = 1.2, \tau_a = 20.0$, resulting in $\langle T \rangle \approx 21.13$. Parameters for both plots: $T = 10^3, \Delta t = 5 \cdot 10^{-4}, N = 10^4, D = 0.1, \Delta = 1.0$.

theory to simulations, where we have deliberately chosen a large kick size of the adaptation Δ. Here, we are in a regime where we do not expect the perturbation stemming from the adaptation to be small and therefore do not expect our theory to hold. We can see that there are artefacts (peaks) appearing at the firing rate and at the *adaptation frequency* $1/\tau_a$. However, the small and large frequency asymptotes are still well described by our theory.

4.3.2 Second order susceptibility

Now let us consider also the second order in the Volterra series, so that our equation for the firing rate states

$$\begin{aligned} r(\omega) = 2\pi r_0 \delta(\omega) &+ \chi_1(\omega;\hat{\mu},D)\left(s(\omega) - a(\omega) + 2\pi\langle a\rangle\delta(\omega)\right) \\ &+ \frac{1}{2\pi}\int d\omega_1 \chi_2(\omega-\omega_1,\omega_1)\left[s(\omega-\omega_1) - a(\omega-\omega_1)\right. \\ &\left.+2\pi\langle a\rangle\delta(\omega-\omega_1))(s(\omega_1) - a(\omega_1) + 2\pi\langle a\rangle\delta(\omega_1)\right] \end{aligned} \tag{4.28}$$

Using the same arguments as in the last section we average over the right side of the equation resulting in

$$r(\omega) = A(\omega)\delta(\omega) + B(\omega)s(\omega) + C(\omega)r(\omega) + \frac{1}{2\pi}\int d\omega_1 \chi_2(\omega-\omega_1,\omega_1)s(\omega-\omega_1)s(\omega_1) + \frac{1}{2\pi}\int d\omega_1 K(\omega,\omega_1)r(\omega_1) \tag{4.29}$$

where we have introduced

$$\Omega(\omega) = \frac{\Delta\tau_a}{1-i\tau_a\omega} \tag{4.30}$$

$$A(\omega) = 2\pi r_0 + 2\pi\langle a\rangle\chi_1(\omega) + 2\pi\langle a\rangle^2\chi_2(0,\omega) + \frac{1}{2\pi}\int d\omega_1 \chi_2(-\omega_1,\omega_1)\frac{\Delta^2\tau_a^2}{1-\tau_a^2\omega_1^2}S_{xx}(\omega_1) \tag{4.31}$$

$$B(\omega) = \chi_1(\omega) + 2\langle a\rangle\chi_2(0,\omega) \tag{4.32}$$

$$C(\omega) = -B(\omega)\Omega(\omega) \tag{4.33}$$

$$K(\omega,\omega_1) = -2\chi_2(\omega-\omega_1,\omega_1)\Omega(\omega_1)s(\omega-\omega_1) \tag{4.34}$$

To bring this expression back into the form of a Volterra series we rearrange the above equation for the firing rate and introduce two new functions

$$r(\omega) = \frac{A(\omega)}{1-C(\omega)}\delta(\omega) + \frac{B(\omega)}{1-C(\omega)}s(\omega) + \frac{1}{2\pi}\int d\omega_1 \frac{\chi_2(\omega-\omega_1,\omega_1)}{1-C(\omega)}s(\omega-\omega_1)s(\omega_1) + \frac{1}{2\pi}\int d\omega_1 \frac{K(\omega,\omega_1)}{1-C(\omega)}r(\omega_1) \tag{4.35}$$

$$:= f(\omega) + \int d\omega_1 g(\omega,\omega_1)r(\omega_1). \tag{4.36}$$

The first three terms look promising, but we still have a problem. Due to the adaptation the firing rate depends on itself through the integral term. However, in rewriting the series with the functions $f(\omega)$ and $g(\omega,\omega_1)$ we can see that our problem has the form of a Fredholm integral equation of second type. We can solve this equation by iteratively inserting $f(\omega)$ into the integral term, yielding approximations of different orders. The full solution is then an infinite sum which is also called a Liouville-Neumann series [29]. Considering only the first two orders results in

$$r^0(\omega) = f(\omega) \tag{4.37}$$

$$r^1(\omega) = f(\omega) + \int d\omega_1 g(\omega,\omega_1)f(\omega_1). \tag{4.38}$$

In the zeroth order we get

$$r^0(\omega) = \frac{A(\omega)}{1-C(\omega)}\delta(\omega) + \frac{B(\omega)}{1-C(\omega)}s(\omega) + \int d\omega_1 \frac{\chi_2(\omega-\omega_1,\omega_1)}{1-C(\omega)}s(\omega-\omega_1)s(\omega_1) \tag{4.39}$$

from which we identify the stationary firing and susceptibilities by comparing with the Volterra series

$$r_0^0 = \frac{A(0)}{1 - C(0)} \tag{4.40}$$

$$\chi_1^0(\omega) = \frac{B(\omega)}{1 - C(\omega)} \tag{4.41}$$

$$\chi_2^0(\omega_1, \omega_2) = \frac{\chi_2^{\mathrm{LIF}}(\omega_1, \omega_2)}{1 - C(\omega_1 + \omega_2)} \tag{4.42}$$

In the first order we get (we neglect all terms of third order in $s(\omega)$)

$$r^1(\omega) = \frac{A(\omega)}{1 - C(\omega)}\delta(\omega) + \left(\frac{B(\omega)}{1 - C(\omega)} - 2\frac{\chi_2(\omega, 0)\Omega(0)A(0)}{(1 - C(\omega))(1 - C(0))} \right) s(\omega) \tag{4.43}$$

$$+ \int d\omega_1 \left(\frac{\chi_2(\omega - \omega_1, \omega_1)}{1 - C(\omega)} - 2\frac{\chi_2(\omega - \omega_1, \omega_1)\Omega(\omega_1)B(\omega_1)}{(1 - C(\omega))(1 - C(\omega_1))} \right) s(\omega - \omega_1)s(\omega_1) \tag{4.44}$$

with the according stationary firing and susceptibilities

$$r_0^1 = \frac{A(0)}{1 - C(0)} \tag{4.45}$$

$$\chi_1^1(\omega) = \frac{B(\omega)}{1 - C(\omega)} - 2\frac{\chi_2(\omega, 0)\Omega(0)A(0)}{(1 - C(\omega))(1 - C(0))} \tag{4.46}$$

$$\chi_2^1(\omega_1, \omega_2) = \frac{\chi_2(\omega_1, \omega_2)}{1 - C(\omega_1 + \omega_2)} - 2\frac{\chi_2(\omega_1, \omega_2)\Omega(\omega_1)B(\omega_1)}{(1 - C(\omega_1 + \omega_2))(1 - C(\omega_1))}. \tag{4.47}$$

Already from an analytical perspective these expressions give us valuable insight into the problem. Since adaptation is a feedback mechanism that couples the output of the neuron (the spike train) to itself, it will naturally lead to a coupling of the different orders of susceptibilities as can be seen for example in the expressions for the second order susceptibilities in (4.42) and (4.47) which feature the first and second order susceptibility with a prefactor $\Omega(\omega)$. A similar effect may be achieved by considering a network model of size one, where the output is fed back into the system as a signal with some weighing function [27].

A check with numerical simulations can be seen in fig. 4.5. First, as in the case of the nonadapting leaky integrate-and-fire model we can clearly see maxima at the firing rate (which is $r_0 \approx 1.5$ in this case). We can also see a maximum for $f_1 + f_2 \approx r_0$, which is the diagonal line from the top left to the bottom right. Second, we can see that the patterns seen in the numerically obtained data are already well featured in the zeroth order approximation, however the magnitude of the absolute value is off as can be seen by the bright yellow. The first order approximation improves the accuracy and we can conclude that it describes the data from the simulations well.

Another interesting comparison is the one between an adapting leaky integrate-and-fire neuron and the according nonadapting leaky integrate-and-fire neuron with a reduced base current. This situation is presented in fig. 4.6. We can see that there is little if any difference between

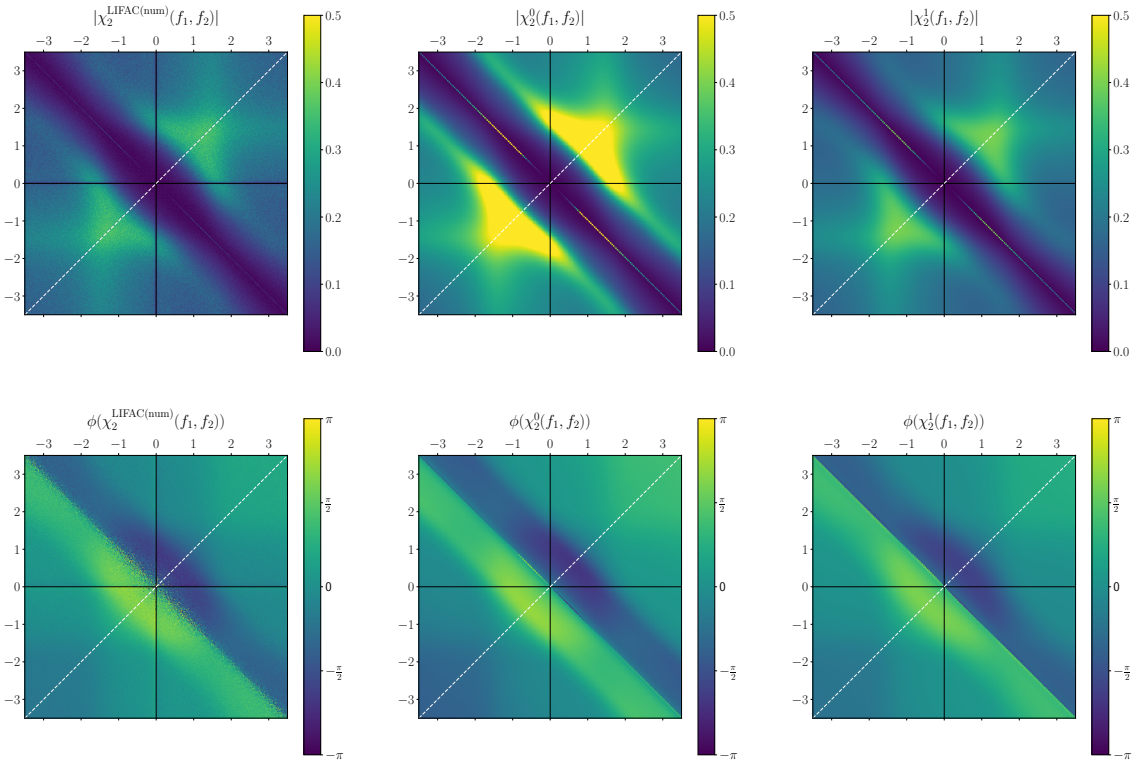

Figure 4.5: Second order susceptibility of the LIFAC: We show the absolute value (top row) and complex angle (bottom row) of the second order susceptibility of an adapting leaky integrate-and-fire neuron. On the left side we show data that has been obtained using the measurement scheme presented in chapter 3, in the middle we show the zeroth order approximation shown in (4.42) and on the right side we calculated the first order approximation using (4.47). We restricted the color bar in the top row to 0.5 for better visibility. Values larger than 0.5 are shown in bright yellow. Parameters: $\mu = 3.5, D = 0.1, \tau_a = 10, \Delta = 0.1, T = 100, \Delta t = 5 \cdot 10^{-3}, N = 10^6$.

the two plots. This implies that, atleast for the parameters shown in the plot and some other feasible to the weakly electric fish, the second order response of the P-units can be approximated well by a nonadapting LIF with a reduced base current. However, one should use the analytic expressions to systematically investigate parameter regimes in which there is indeed a significant difference between the adapting and nonadapting LIF.

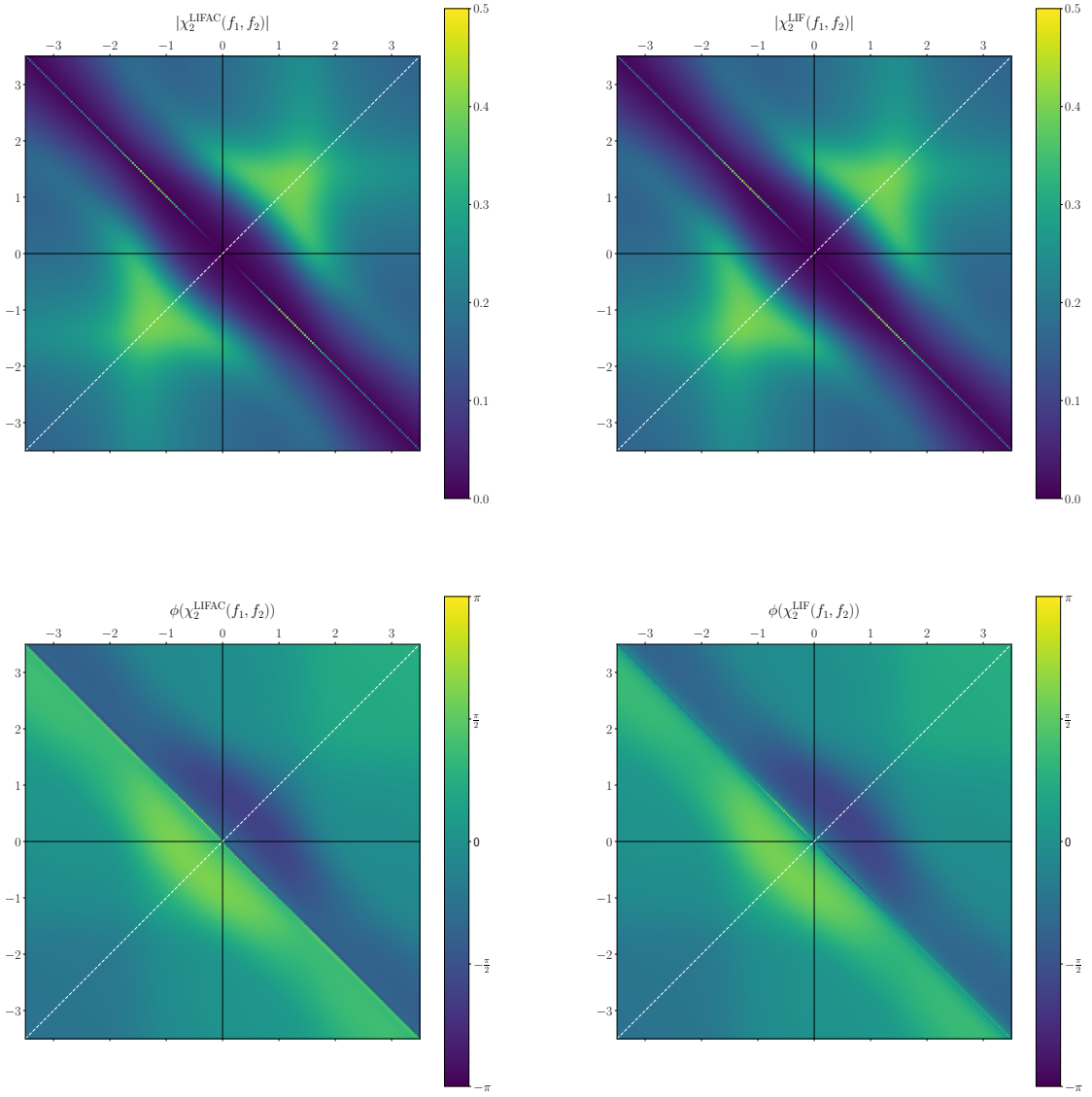

Figure 4.6: Comparison χ_2^{LIFAC} vs. χ_2^{LIF}: We compare the second order susceptibility of an adapting leaky integrate-and-fire neuron with the analog nonadapting leaky integrate-and-fire neuron with a reduced base current. Parameters LIFAC: $\mu = 3.5, D = 0.1, \tau_a = 10, \Delta = 0.1$, Parameters LIF: $\mu = 1.99, D = 0.1$, other Parameters: $T = 100, \Delta t = 5 \cdot 10^{-3}, N = 10^6$.

CHAPTER 5

Spike: A numerical toolbox for integrate-and-fire simulations

In the previous chapters we have shown lots of plots comparing our analytical results to numerical simulations. However, without a closer look at how we did said simulations the comparison is meaningless. We will present the software used throughout the thesis in this chapter and show which assumptions underly its numerical work.

5.1 Project description

The name of the software project is Spike and it is written in C++ and is freely avaiable at github.com/chegerland/spike. Spike is specifically written for the numeric measurement of susceptibilities of integrate-and-fire neurons, but we may also calculate phase plane trajectories and firing rates with it. It is a library implementing lots of functionalities with several executables that do the heavy lifting and have all been written to work on a cluster using MPI.

In chapter chapter 3 we have already outlined the numeric scheme with which we measure the susceptibilities

- Prepare white noise signal $x(t)$ with variance A
- Simulate neuron model with the white noise as input
- Measure the output, i.e. the spike train $y(t)$
- Use formulae (3.9) and (3.13) to obtain the susceptibilities

We will outline each of these steps since they all come with their own difficulties. We choose a time frame of length T and a time step Δt, which fully determine our time discretization. The discrete times are then given by

$$t_k = t_0 + k\Delta t, k = 0, 1, 2, \dots, N-1 \tag{5.1}$$

$$N = \frac{T}{\Delta t} = \frac{t_{\text{end}} - t_0}{\Delta t} \tag{5.2}$$

and may be represented as an array of length N.

5.2 Generating gaussian white noise

We need a discretized version of gaussian white noise with variance A. We prepare a complex number array `f[n]` of length N and fill every entry in the following way

```
f[n] = sqrt(A * T) * (cos(2 * pi * rand) + I * sin(2 * pi * rand))
```

where `rand` is a random number drawn from a normal distribution with mean zero and standard deviation of one. The prefactor ensures that the variance of the gaussian white noise is indeed equal to A, we can see this by evaluating the power spectrum, which is

```
S[n] = 1/T * f[n] * conj(f[n]) = 1/T * sqrt(A * T) * sqrt(A * T) = A
```

where we omitted the array index and wrote `conj(f)` for the complex conjugated frequency. This frequency spectrum of the gaussian white noise has to be cut off at the highest frequency of the system, which, in our case, is the Nyquist frequency $1/(2\Delta t)$. Cut off means, that all frequencies higher than the Nyquist frequency are simply set to zero. The resulting frequency array is then Fourier transformed using a fast Fourier transform method, which gives us the gaussian white noise in time domain.

5.3 Simulating adapting integrate-and-fire neurons

For the simulation of an (adapting) integrate-and-fire neuron we choose the same time discretization as above. Then we use the Euler-Maruyama method to get an approximate solution to the stochastic differential equation. In the case of an adapting integrate-and-fire neuron we simply include the adaptation current in the process as we would do in a nonstochastic Euler method. Let us take as an example the adapting leaky integrate-and-fire neuron with the parameters μ, D, Δ, τ_a. The simulation with a signal looks something like this

```
 for (i = 1; i < N; i++) {
   v[i] = v[i-1]  + (mu - v[i-1] - a + s[i-1]) * dt
                  + sqrt(2*D) * rand * sqrt(dt)
   a[i] = a[i-1] - 1 / tau_a * a[i-1] * dt

   if (v[i] > 1) {
     v[i] = 0
     a[i] += Delta
   }
}
```

where `rand` is again a random number drawn from a normal distribution with mean zero and standard deviation of one, and we have named all parameters like their LaTeX equivalents. In the last four lines of the code we see the fire-and-reset rule. With this simulation method it is easy to construct a spike train: Take an array of length `N`, every time the neuron does not spike the according entry is zero, everytime it does spike the entry is `1/dt`.

5.4 Numerical measurement of the susceptibilities, FFT

Now that we know how to numerically represent the spike train and the input signal, which is gaussian white noise, we may proceed by calculating the susceptibilities. As presented in

chapter 3 we may calculate them with these formulae

$$\chi_1(\omega) = \frac{S_{xs}(\omega)}{A} \tag{5.3}$$

$$\chi_2(\omega_1, \omega_2) = \frac{S_{xss}(\omega)}{2A^2} \tag{5.4}$$

where $S_{xs}(\omega)$ and $S_{xss}(\omega_1, \omega_2)$ are the (higher order) cross spectra between the spike train x and the signal s. Mathematically they are defined as Fourier transform of an appropriate cross correlation function. Numerically we can approximate them by their finite time counter parts

$$S_{xs}(\omega) = \lim_{T\to\infty} \tilde{S}_{xs}(\omega) = \frac{1}{T}\int_0^T x(t)\exp(-i\omega t)dt \int_0^T s(t')\exp(i\omega t')dt \tag{5.5}$$

$$\begin{aligned} S_{xss}(\omega_1, \omega_2) &= \lim_{T\to\infty} \tilde{S}_{xss}(\omega_1, \omega_2) \\ &= \frac{1}{T}\int_0^T x(t)\exp(-i(\omega_1+\omega_2)t)dt \\ &\quad \int_0^T s(t')\exp(i\omega_1 t')dt' \int_0^T s(t'')\exp(i\omega_2 t'')dt'' \end{aligned} \tag{5.6}$$

Notice that the normalization factor for the higher order cross spectrum is still $1/T$ [30]! As we can see from the limit in the last expression our time window has to be large for the approximation to be valid. We approximate the integral $\int_0^T x(t)\exp(-i\omega t)dt$ by employing our time discretization from before, resulting in

$$x(\omega) = \int_0^T x(t)\exp(-i\omega t)dt \approx \Delta t \sum_{k=0}^{N-1} x_k \exp(-i\omega_n t_k) = x(\omega_n), \tag{5.7}$$

with the discrete, positive frequencies $\omega_n = 2\pi n/T, n = 0, 1, \ldots, N/2$. The sum

$$\sum_{k=0}^{N-1} x_k \exp(-i\omega_n t_k) \tag{5.8}$$

can be calculated very fast using a fast Fourier transform (FFT) algorithm.

In the simulation the first order susceptibility will be a one dimensional array, whereas the second order susceptibility will be a two dimensional array. In both cases each entry will correspond to a specific, positive frequency or in the case of the second order susceptibility a combination of positive frequencies. To get the whole frequency range, i.e. positive and negative frequencies we may use the following symmetry relations, that are evident from the definitions of the (higher order) cross spectra

$$\chi_1(-\omega) = \chi_1^*(\omega) \tag{5.9}$$

$$\chi_2(\omega_1, \omega_2) = \chi_2(\omega_2, \omega_1) \tag{5.10}$$

$$\chi_2(-\omega_1, -\omega_2) = \chi_2^*(\omega_1, \omega_2) \tag{5.11}$$

Contrary to [2] this does not mean that the first quarter fully determines the second order susceptibility for the whole frequency range, but it rather implies that we may only calculate one triangle of the first and one triangle of the fourth quarter as shown in fig. 5.1.

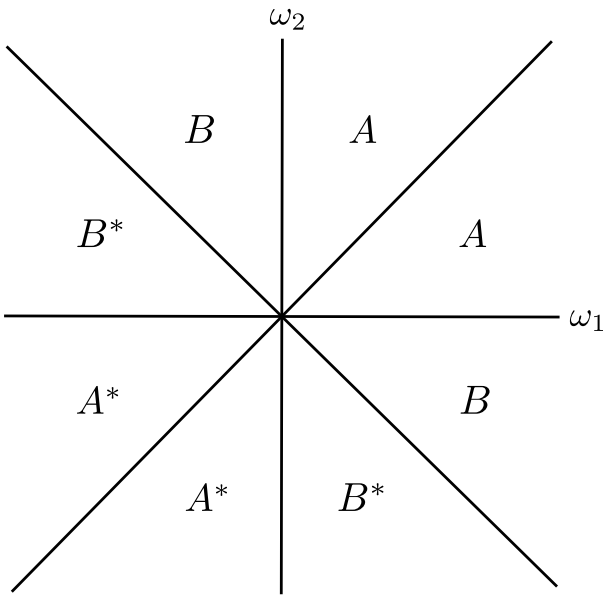

Figure 5.1: Using symmetries of the second order susceptibility we may restrict our calculation to two principal domains A and B.

CHAPTER 6

Outlook

In chapter 2 we have calculated the second order susceptibility for a general integrate-and-fire neuron and we have shown that we can reduce it to the known case of a leaky integrate-and-fire neuron. Our work would greatly benefit from a further calculation for e.g. the perfect or quadratic integrate-and-fire models, especially for comparison between the models as has been done in [26]. Whether it is possible to obtain analytic expressions has to be shown, but even a numerical treatment and comparison is likely to be fruitful. A known method for the numeric calculation of the response functions is the Richardson threshold integration method [31] could be adapted for the calculation of the second order susceptibility. It may also be constructive since it provides an alternative numerical approach to the one we have presented in chapter 5.

In chapter 3 we have inspected the parametric dependency of the first and second order susceptibility on the noise strength. We have shown that the susceptibilities depend on the sum of the intrinsic and external noise strength. The arguments that we have presented may be readily applied to all higher order susceptibilities.

Then in chapter 4 we have finally calculated the first and second order susceptibility for the adapting leaky integrate-and-fire neuron. The expressions have been obtained in the limit of a slow and weak adaptation. Whether they actually describe the nonlinear response in the P-unit of the weakly electric fish has to be checked by experiment of course. On a theoretical level we noticed that the obtained expression for the adapting leaky integrate-and-fire neuron does not significantly differ from the nonadapting leaky integrate-and-fire neuron with a reduced base current. This may be due to the parameters we have used and future work should explore whether this phenomenon is universal or, in other words, for which parameters there is a significant difference between the two. In any case we have used a self consistent approach to obtain analytical expressions that match well with the numerically obtained data.

Finally, in chapter 5 we have shown how we carry out our numeric simulations. We concluded that the main difficulties are that we need a long time window, short time steps and a lot of realizations in order for our results to be accurate. Thanks to the parallelization of our code we are able to run simulations on a computer cluster, which greatly accelerates the process of obtaining numerical data.

Bibliography

1. S. O. Voronenko and B. Lindner, “Weakly Nonlinear Response of Noisy Neurons", en. New Journal of Physics **19,** 033038 (2017).
2. S. O. Voronenko, “Nonlinear Signal Processing by Noisy Spiking Neurons", en (2018).
3. E. I. Knudsen, “Spatial Aspects of the Electric Fields Generated by Weakly Electric Fish", en. Journal of comparative physiology **99,** 103 (1975).
4. L. Chen, J. L. House, R. Krahe and M. E. Nelson, “Modeling Signal and Background Components of Electrosensory Scenes", en. Journal of Comparative Physiology A **191,** 331 (2005).
5. J. Henninger, R. Krahe, F. Kirschbaum, J. Grewe and J. Benda, “Statistics of Natural Communication Signals Observed in the Wild Identify Important Yet Neglected Stimulus Regimes in Weakly Electric Fish", en. Journal of Neuroscience **38,** 5456 (2018).
6. M. Savard, R. Krahe and M. Chacron, “Neural Heterogeneities Influence Envelope and Temporal Coding at the Sensory Periphery", en. Neuroscience **172,** 270 (2011).
7. M. J. Chacron, A. Longtin and L. Maler, “Simple Models of Bursting and Non-Bursting P-Type Electroreceptors", en. Neurocomputing **38-40,** 129 (2001).
8. M. J. Chacron, A. Longtin and L. Maler, “Negative Interspike Interval Correlations Increase the Neuronal Capacity for Encoding Time-Dependent Stimuli", en. The Journal of Neuroscience **21,** 5328 (2001).
9. M. J. Chacron, A. Longtin and L. Maler, “To Burst or Not to Burst?", en. Journal of Computational Neuroscience **17,** 127 (2004).
10. M. Beiran, A. Kruscha, J. Benda and B. Lindner, “Coding of Time-Dependent Stimuli in Homogeneous and Heterogeneous Neural Populations", en. Journal of Computational Neuroscience **44,** 189 (2018).
11. J. Henninger, R. Krahe, F. Sinz and J. Benda, “Tracking Activity Patterns of a Multi-species Community of Gymnotiform Weakly Electric Fish in Their Neotropical Habitat without Tagging", en. Journal of Experimental Biology **223** (2020).
12. J. H. McDermott, “The Cocktail Party Problem", en. Current Biology **19,** R1024 (2009).
13. T. Schwalger, “The Interspike-Interval Statistics of Non-Renewal Neuron Models", eng (2013).
14. T. Schwalger and B. Lindner, “Patterns of Interval Correlations in Neural Oscillators with Adaptation", English. Frontiers in Computational Neuroscience **7** (2013).
15. V. Volterra, *Theory of Functionals and of Integral and Integro-Differential Equations*. eng (Dover Publications, Mineola, N.Y, 2005).
16. N. Wiener, *Nonlinear Problems In Random Theory Norbert Wiener*. eng (1958).

17. Y. W. Lee and M. Schetzen, “Measurement of the Wiener Kernels of a Non-Linear System by Cross-Correlation", International Journal of Control **2,** 237 (1965).
18. S. Orcioni, “Improving the Approximation Ability of Volterra Series Identified with a Cross-Correlation Method", en. Nonlinear Dynamics **78,** 2861 (2014).
19. B. Lindner, *Neural Noise Script* (2018).
20. B. Lindner and L. Schimansky-Geier, “Transmission of Noise Coded versus Additive Signals through a Neuronal Ensemble", Physical Review Letters **86,** 2934 (2001).
21. N. Brunel, F. S. Chance, N. Fourcaud and L. F. Abbott, “Effects of Synaptic Noise and Filtering on the Frequency Response of Spiking Neurons", Physical Review Letters **86,** 2186 (2001).
22. A. S. French and E. G. Butz, “Measuring the Wiener Kernels of a Non-Linear System Using the Fast Fourier Transform Algorithm", International Journal of Control **17,** 529 (1973).
23. J. Benda, L. Maler and A. Longtin, “Linear Versus Nonlinear Signal Transmission in Neuron Models With Adaptation Currents or Dynamic Thresholds", Journal of Neurophysiology **104,** 2806 (2010).
24. B. Lindner and A. Longtin, *Nonrenewal Spike Trains Generated by Stochastic Neuron Models Noise in Complex Systems and Stochastic Dynamics* **5114** (International Society for Optics and Photonics, 2003), 209.
25. Y.-H. Liu and X.-J. Wang, “Spike-Frequency Adaptation of a Generalized Leaky Integrate-and-Fire Model Neuron", en. Journal of Computational Neuroscience **10,** 25 (2001).
26. R. D. Vilela and B. Lindner, “Comparative Study of Different Integrate-and-Fire Neurons: Spontaneous Activity, Dynamical Response, and Stimulus-Induced Correlation", Physical Review E **80,** 031909 (2009).
27. B. Lindner, B. Doiron and A. Longtin, “Theory of Oscillatory Firing Induced by Spatially Correlated Noise and Delayed Inhibitory Feedback", en. Physical Review E **72,** 061919 (2005).
28. J. Benda and A. V. M. Herz, “A Universal Model for Spike-Frequency Adaptation", eng. Neural computation, 2523 (2003).
29. Arfken, *Mathematical Methods for Physicists*. en (Elsevier, 2013).
30. C. L. Nikias and A. P. Petropulu, *Higher-Order Spectra Analysis: A Nonlinear Signal Processing Framework* (PTR Prentice Hall, Englewood Cliffs, N.J, 1993).
31. M. J. E. Richardson, “Spike-Train Spectra and Network Response Functions for Non-Linear Integrate-and-Fire Neurons", en. Biological Cybernetics **99,** 381 (2008).

Acknowledgments

Since the majority of this thesis has been prepared amidst a global pandemic, an event which has profoundly influenced me and therefore this work, I would first like to acknowledge those that have helped me maintain my sanity and mental health during these times. My girlfriend Gerda, my parents and their partners, my grandparents, my friends and my cat Coco have all helped me cope with the isolation and kept up my spirits.

I am of course deeply indebted to Prof. Benjamin Lindner, for giving me the oppurtunity to work on such an interesting problem, as well as (if not more so) for the tight supervision during the whole project. Our weekly meetings were a healthy back-and-forth between two inquisitive people that have led me to many great insights and a deeper focus on understanding the topic at hand.

Last but not least I would like to thank Paul Ledwon and Konstantin Holzhausen in particular for proofreading parts of the thesis.

Thank you all!

Ich erkläre, dass ich die vorliegende Arbeit selbständig verfasst und noch nicht für andere Prüfungen eingereicht habe. Sämtliche Quellen einschließlich Internetquellen, die unverändert oder abgewandelt wiedergegeben werden, insbesondere Quellen für Texte, Grafiken, Tabellen und Bilder, sind als solche kenntlich gemacht. Mir ist bekannt, dass bei Verstößen gegen diese Grundsätze ein Verfahren wegen Täuschungsversuchs bzw. Täuschung eingeleitet wird.

Berlin, den 26. Februar 2021